UNIVERSITY OF JYVÄSKYLÄ
DEPARTMENT OF CHEMISTRY

RESEARCH REPORT NO. 160

KARI AHONEN

SOLID STATE STUDIES OF PHARMACEUTICALLY IMPORTANT MOLECULES AND THEIR DERIVATIVES

Academic Dissertation for
the Degree of Doctor of Philosophy

UNIVERSITY OF JYVÄSKYLÄ
2012

DEPARTMENT OF CHEMISTRY, UNIVERSITY OF JYVÄSKYLÄ
RESEARCH REPORT No. 160

SOLID STATE STUDIES OF PHARMACEUTICALLY IMPORTANT MOLECULES AND THEIR DERIVATIVES

BY

KARI AHONEN

Academic Dissertation for the Degree of
Doctor of Philosophy

To be presented, by permission of the Faculty of Mathematics and Science of the University of Jyväskylä, for public examination in Auditorium KEM1, on December 1st 2012, at 10 o'clock.

UNIVERSITY OF JYVÄSKYLÄ

Jyväskylä, Finland
ISBN 978-951-39-4965-5
ISSN 0357-346X; 160

URN:ISBN:978-951-39-9967-4
ISBN 978-951-39-9967-4 (PDF)

Jyväskylän yliopisto, 2024

ABSTRACT

Ahonen, Kari
Solid state studies of pharmaceutically important molecules and their derivatives
Jyväskylä: University of Jyväskylä, 2012, 65 p.
(Department of Chemistry, University of Jyväskylä, Research Report Series
ISSN 0357-346X; 160)
ISBN 978-951-39-4965-5

The research described in this thesis provides important information about the solid state behavior of amides of bile acids with potential pharmaceutical activity. Polymorph/solvate screening and structural characterization for nine bile acid derivatives consisting of bile acids with varying amounts of hydroxyl groups and a selection of small molecules combined via an amide linkage was performed. Two of the studied compounds were shown to be polymorphic, and hydrates/solvates were identified for six amides. Detailed structural characterization for the isolated solid state forms was performed using a wide selection of experimental methods, including single crystal and powder X-ray diffraction, solid state NMR spectroscopy, optical spectroscopy, and thermoanalytical methods. Information about the solid state structures of molecules with potential pharmaceutical activity is important, since different crystal forms may possess different chemical, physical, and pharmaceutical properties.

Infinite crystal calculations were conducted for a series of three nitrogen heterocycles in order to compare the single crystal structures to SS-NMR data. Optimization of hydrogen atom positions was proven to be essential to reproduce the solid state NMR chemical shielding data starting from single crystal X-ray structures. Moreover, the ability of the NMR-CASTEP program to reliably predict SS-NMR chemical shifts for nitrogen heterocycles was demonstrated.

Pharmacological applications of aminopyridines, basic aspects of polymorphism and its significance in pharmacology, and analytical methods in crystal form characterization are briefly summarized in the literature review.

Keywords: bile acid, aminopyridine, solid state structural analysis, polymorphism, infinite crystal calculations

Author's address

Kari Ahonen
University of Jyväskylä
Department of Chemistry
P.O. Box 35, FI-40014
University of Jyväskylä
Finland
ahonenkva@yahoo.com

Supervisors

Adjunct Professor Elina Sievänen
Department of Chemistry
University of Jyväskylä
Finland

Professor Emeritus Erkki Kolehmainen
Department of Chemistry
University of Jyväskylä
Finland

Reviewers

Dr. Jaroslav Havlíček
Zentiva a.s.
Prague, Czech Republic

Professor Urszula Rychlewska
Department of Chemistry
Adam Mickiewicz University
Poznań, Poland

Opponent

Professor Jouko Vepsäläinen
Department of Biosciences
University of Eastern Finland
Kuopio, Finland

PREFACE

This research was conducted at the Department of Chemistry of the University of Jyväskylä, Finland, and at the Institute of Organic Chemistry and Biochemistry of the Academy of Sciences of the Czech Republic, from February 2009 to summer 2012.

I am thankful to everyone who has positively influenced this doctoral thesis. Financial support was provided by the Academy of Finland, the Academy of Sciences of the Czech Republic, and the University of Jyväskylä.

Kerava 12.9.2012
Kari Ahonen

LIST OF ORIGINAL PUBLICATIONS

I K. Ahonen, B. Behera, E. Sievänen, A. Valkonen, M. Lahtinen, M. Tolonen, R. Kauppinen, and E. Kolehmainen, Structural studies on lithocholyl-*N*-(2-aminoethyl)amide in the solid state, *Struct. Chem.*, **2010**, *21*, 185-190.
https://doi.org/10.1007/s11224-009-9560-7

II K. V. Ahonen, M. Lahtinen, A. Valkonen, M. Dračinský, and E. Kolehmainen, Microwave assisted synthesis and solid-state characterization of lithocholyl amides of isomeric aminopyridines, *Steroids*, **2011**, *76*, 261-268.
https://doi.org/10.1016/j.steroids.2010.11.007

III K. V. Ahonen, M. Lahtinen, M. Löfman, A. Kiesilä, A. Valkonen, E. Sievänen, Nonappa, and E. Kolehmainen, Structural studies of five novel bile acid-4-aminopyridine conjugates, *Steroids*, **2012**, *77*, 1141-1151.
https://doi.org/10.1016/j.steroids.2012.06.003

IV M. Dračinský, P. Jansa, K. Ahonen, and M. Buděšinský, Tautomerism and the protonation/deprotonation of isocytosine in liquid- and solid-states studied by NMR spectroscopy and theoretical calculations, *Eur. J. Org. Chem.*, **2011**, 1544-1551.
https://doi.org/10.1002/ejoc.201001534

V B. Ośmiałowski, E. Kolehmainen, S.-M. Ikonen, K. Ahonen, and M. Löfman, NMR crystallography of 2-acylamino-6-[1*H*]-pyridones: solid state NMR, GIPAW computational, and single crystal X-ray diffraction studies, *J. Mol. Struct.*, **2011**, *1006*, 678-683.
https://doi.org/10.1016/j.molstruc.2011.10.034

From articles IV and V, only synthesis, solid state NMR, and infinite crystal calculations are included to this thesis.

ABBREVIATIONS

4M2AP	4-methyl-2-aminopyridine
AA	arachidonic acid
AChE	acetylcholinesterase
AP	aminopyridine
BA	bile acid
BBB	blood-brain barrier
BFGS	Broyden-Fletcher-Goldfarb-Shanno
CA	cholic acid
CASTEP	Cambridge Serial Total Energy Package
CDCA	chenodeoxycholic acid
CHK2	checkpoint kinase 2
COX	cyclooxygenase
CRC	colorectal cancer
CSA	chemical shift anisotrophy
DCA	deoxycholic acid
DFT	density functional theory
DSC	differential scanning calorimetry
FDA	U.S. Food and Drug Administration
FSLG-HETCOR	frequency-switched Lee–Goldburg heteronuclear correlation
GIPAW	gauge-including projector-augmented wave
GKA	glucokinase activator
HIV	human immunodeficiency virus
HD	Huntington's disease
HEN	heterogeneous nucleation
HON	homogeneous nucleation
HT	high-throughput
ICH	International Committee on Harmonization
LCA	lithocholic acid
LEMS	Lambert-Eaton myasthenic syndrome
MG	myasthenia gravis
MS	multiple sclerosis
MW	microwave
NAD^+	nicotinamide adenine dinucleotide
NOS	nitric oxide syntase
NSAID	non-steroidal anti-inflammatory drug
NQS	non-quaternary suppression
OATP	organic anion transporting polypeptide
PBC	primary biliary cirrhosis
PG	prostaglandin
PI3K/Akt	phosphatidylinositol 3-kinase/protein kinase B
PSC	primary sclerosing cholangitis
SCA1	spinocerebellar ataxia type 1

SCI	spinal cord injury
SSB	spinning side band
SS-NMR	solid state nuclear magnetic resonance
T2DM	type 2 diabetes mellitus
TEA	triethylamine
TG	thermogravimetry
THF	tetrahydrofuran
UDCA	ursodeoxycholic acid
XRD	X-ray diffraction

CONTENTS

1 BIOLOGICAL AND PHARMACOLOGICAL PROPERTIES OF AMINOPYRIDINES AND BILE ACIDS

1.1 2-Aminopyridine and its derivatives

The main use of 2-aminopyridine (2-AP) is as an intermediate in the manufacture of a variety of pharmaceuticals.[1] It is convulsant in humans and lethal amounts can be absorbed through the skin.[2] In the following paragraphs, oxicams and antihistamines including 2-AP motif are discussed, followed by an introduction to other biologically active 2-AP derivatives.

Oxicams are a group of non-steroidal anti-inflammatory drugs (NSAIDs) with an enolic acid functionality and a prolonged elimination half-life compared to traditional NSAIDs.[3] NSAIDs are cyclooxygenase (COX) inhibitors that metabolize arachidonic acid (AA) to prostaglandin (PG) H_2 (Scheme 1).[4] PGH_2 is further converted to different PGs including PGE_2, which is primarily associated with inflammation.[5] COX-1 is constantly expressed in nearly all cell types, whereas expression of the COX-2 isoform is induced as a response to cellular stress.[6] However, COX-2 is expressed in constant levels in some organs including certain areas of human brains.[6,7] Unlike other NSAIDs, oxicams activate the phosphatidylinositol 3-kinase/protein kinase B (PI3K/Akt) signaling pathway in human neuroblastoma cells[8], a potential target in the treatment of Parkinson's disease (PD).[9]

Piroxicam (Feldene®, **1**) came into the U.S. market in 1982 and was Pfizer's best-selling drug in the late 1980s.[10] The oral tablet form is mainly used for the symptomatic treatment of osteoarthritis and rheumatoid arthritis[11], and the topical gel formulation is used in the treatment of pain conditions such as sprains and strains.[12] It is suggested to be re-absorbed via enterohepatic circulation[13], although the multiple peak absorption mechanism has not been confirmed.[14] The efficacy/safety profile of piroxicam has been evaluated to be equal or even more favorable than that of traditional NSAIDs.[15] Piroxicam is a

non-selective COX inhibitor with preference for the COX-1 isoform.[16,17] Inducible isoform COX-2[18] is considered a potential target in cancer chemoprevention[19] and treatment[20], and piroxicam has shown to be potent against colon cancer[21,22] and urinary bladder cancer.[23] Currently it is used as a veterinary drug against a variety of cancers.[24,25] In addition, piroxicam has recently been studied for the acute management of migraine.[26] Although piroxicam is relatively well tolerated[15], it has gastrointestinal side effects[27] and consequently several prodrugs have been developed to avoid these drawbacks.

Ampiroxicam (**2**) is inactive as a COX inhibitor but is activated after the stomach, thereby avoiding adverse effects. The stability of the prodrug plays an essential role, since the too-labile droxicam (**3**) releases piroxicam in the stomach and the too-stable pivoxicam (**4**) does not completely metabolize before systemic circulation.[28]

In addition, piroxicam derivatives have been studied and developed for COX-2 inhibition over that of COX-1. As an example, the sulfonate derivative **5** has a two-fold selectivity for COX-2 over COX-1.[29] Tenoxicam (Mobiflex®, **6**) has been shown to have slightly better efficacy and safety profiles than piroxicam.[30] In order to avoid gastrointestinal irritation, transdermal self-adhesive films have been developed for tenoxicam.[31] Furthermore, neuroprotective properties have been observed.[32,33] Lornoxicam (Xefo®, **7**) came into the market in 1995, and was available in parenteral and oral formulations.[34] It is more effective in relieving acute pain than tenoxicam[35] and, unlike oxicams in general, it has a relatively short half-life.[36] Its efficacy is similar to that of morphine with reduced side effects in the treatment of postoperative pain.[37,38] Because of the extremely bitter taste of lornoxicam, a taste-masking formulation has recently been developed, where the drug is only released in the acidic conditions of the stomach.[39] Cinnoxicam (Sinartrol®, **8**) has been studied for male infertility problems as a single agent[40] and in combination with L-carnitine and acetyl-L-carnitine.[41] It is hydrolyzed in acidic conditions to piroxicam.[42] The structures of oxicams **1** - **8** with a 2-AP moiety are presented in Figure 1.

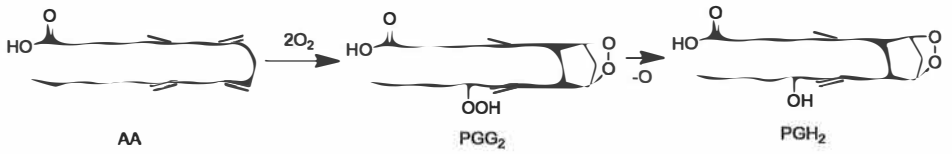

Scheme 1. COX catalyzed synthesis of prostaglandins from arachidonic acid.

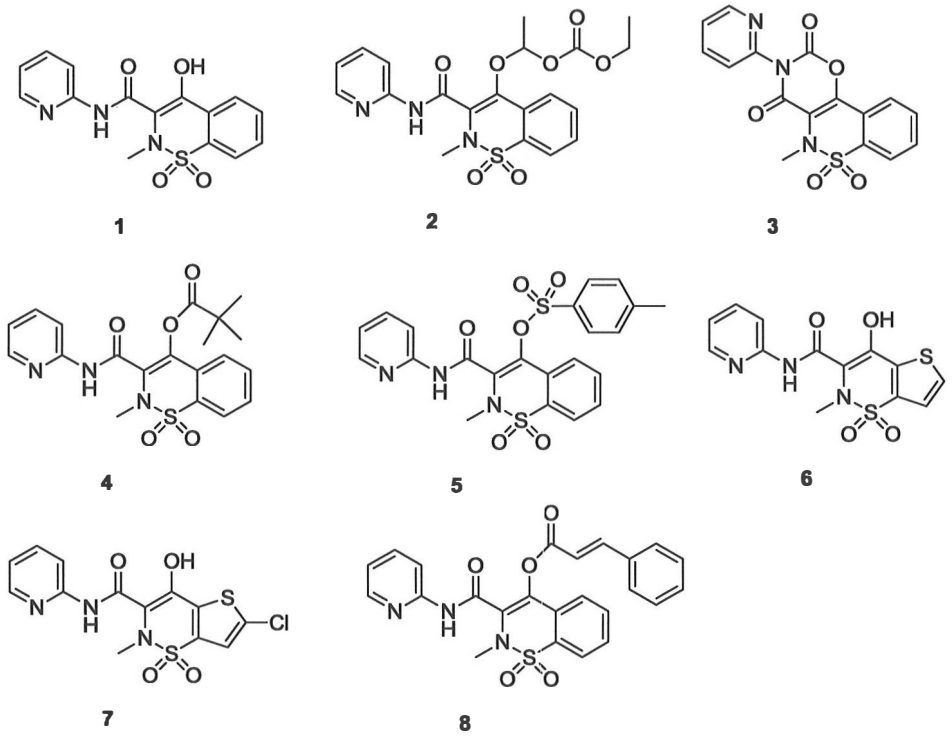

Figure 1. Oxicams with 2-AP moiety.

Pyrilamine (mepyramine, neoartergan, 2786 R.P., **9**)[43] and tripelennamine (**10**) are H_1-receptor antagonists (antihistamines).[44,45] These first-generation antihistamines pass the blood-brain barrier (BBB), causing sedative side effects[46]. Tripelennamine has been misused intravenously in combination with pentazocine ("T's and blues")[47], or with paregoric, heroin, or morphine ("blue velvet")[48] for narcotic purposes. Both of these pharmaceuticals are also used in veterinary medicine and are classified as doping substances in horse and camel races.[49,50] Antihistamines inactivate the H_1-receptors and, from a mechanistic point of view, is has been suggested that the term "antagonist" should be replaced with the term "inverse agonist".[46] Four histamine receptors are known to date and the H_1-receptor is involved in many pathological processes of allergy.[45] ^{3}H-enriched pyrilamine[45], as well as a higher affinity ligand, ^{125}I-iodobolpyramine[51] (**11**), and an irreversible ligand, ^{125}I-iodoazidophenpyramine[52] (**12**), have been used to identify the H_1-receptor distribution in mammalian tissues. The structures of compounds **9 – 12** possessing affinity to the H_1-receptor and including a 2-AP moiety are described in Figure 2.

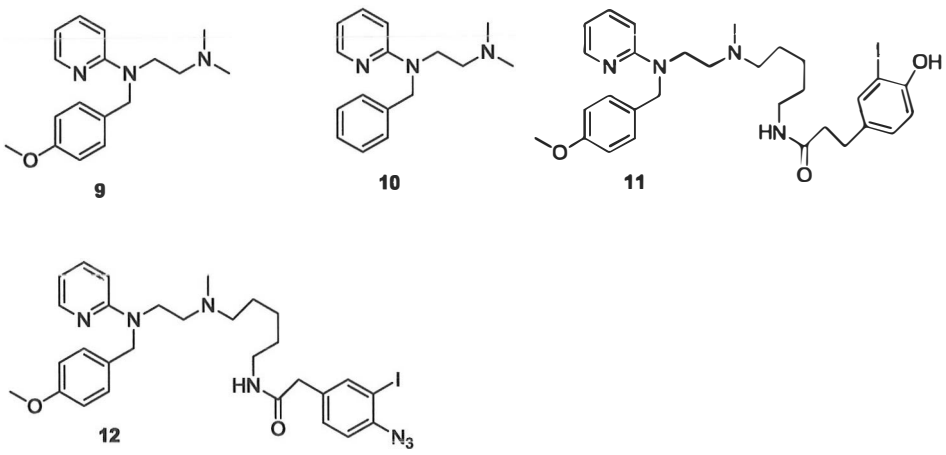

Figure 2. Compounds with affinity to the H_1-receptor with 2-AP moiety.

In vitro and *in silico* studies have been conducted to evaluate 2-aminopyridine derivatives as acetylcholinesterase (AChE) inhibitors, neuroprotective agents[53], and neuronal nitric oxide synthase (nNOS) inhibitors.[54] Several AChE inhibitors are in clinical use for symptomatic treatment of Alzheimer's disease (AD)[55] and 2-aminopyridine-3,5-dicarbonitrile derivatives represent a new potential group with this kind of activity[53] (e.g., compound **13** shows selectivity over BuChE inhibition and neuroprotection of 36 % in human neuroblastoma cells at 1 μM).

Checkpoint kinase 2 (CHK2) regulates the transcription factor E2F-1, which induces the cell cycle arrest and apoptosis in response to DNA damage. As a therapeutic target, blocking CHK2 activity is considered to reduce functioning of E2F-1 and to make cancer cells more sensitive to chemotherapy.[56] High throughput screening of 2-aminopyridine derivatives as CHK2 inhibitors has been conducted; for example, compound **14** showed an IC_{50} value of 92 (±18) nM against CHK2.[57]

Glucokinase activators (GKAs) are a new group of compounds being studied for the treatment of type 2 diabetes mellitus (T2DM). Glucokinase (GK, hexokinase D) has a central role in glucose homeostasis in humans via two separate mechanisms. In the pancreatic β-cells phosphorylation of D-glucose by GK activates secretion of insulin and in the parenchymal cells of the liver insulin activates GK via a hepatic promoter of the GK gene to regulate glycogen synthesis and hepatic glucose production.[58] GKAs GKA50 (**15**) and GKA60 (**16**), developed by Astra Zeneca, have shown high efficacy *in vivo*. Unfortunately, these compounds have epididymal and testicular toxicity and therefore have no clinical value.[59] GKAs can cause hypoglycemia due to GK activation in the pancreas and therefore hepatoselective GKA (**17**) has been developed by Pfizer. This compound is currently under clinical evaluation. It is designed to have low passive permeability and to act as a substrate for the organic anion transporting

polypeptides (OATPs) showing over 50-fold liver/pancreas ratio of tissue distribution.[60]

Nitric oxide (NO) is mainly synthesized in living organisms from L-arginine catalyzed by NO synthases (NOSs) (Scheme 2).[61,62] Three isoforms of NOSs are known, namely constitutive endothelium- and neuronal NOSs (eNOS and nNOS, respectively), as well as an inducible isoform, iNOS. NO has a wide variety of physiological signaling functions including cardiovascular homeostasis and neuronal signaling. In addition, iNOS releases large quantities of NO during inflammation and immunological defence.[62] Because of the overproduction of NO by iNOS, it has been linked to neurodegenerative disorders, multiple sclerosis, stroke, cancer, as well as to many inflammatory diseases, specific iNOS inhibitors are highly eligible.[63] 4-Methyl-2-aminopyridine (4M2AP, **18**) is the most potent NOS inhibitor among the methylated 2-AP derivatives[64], having a modest preference for iNOS over the other isozymes.[65] The 6-propyl derivative of 4M2AP (**19**), for one, has around 10 times higher potency than 4M2AP (IC_{50}, iNOS = 15 nM, eNOS = 34 nM, nNOS = 23 nM). Furthermore, an iNOS selective inhibitor (**20**) has been developed (IC_{50}, iNOS = 79 nM, eNOS >100 μM, nNOS = 6.3 μM).[63] The structures of biologically active molecules **13** – **20** with a 2-AP moiety are depicted in Figure 3.

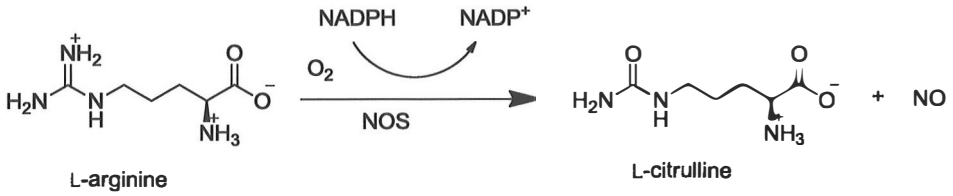

Scheme 2. NO synthesis from L-arginine catalyzed by NOS. Isozymes eNOS and nNOS are Ca^{2+}-dependent, whereas iNOS is activated by cytokines and endotoxins.[62]

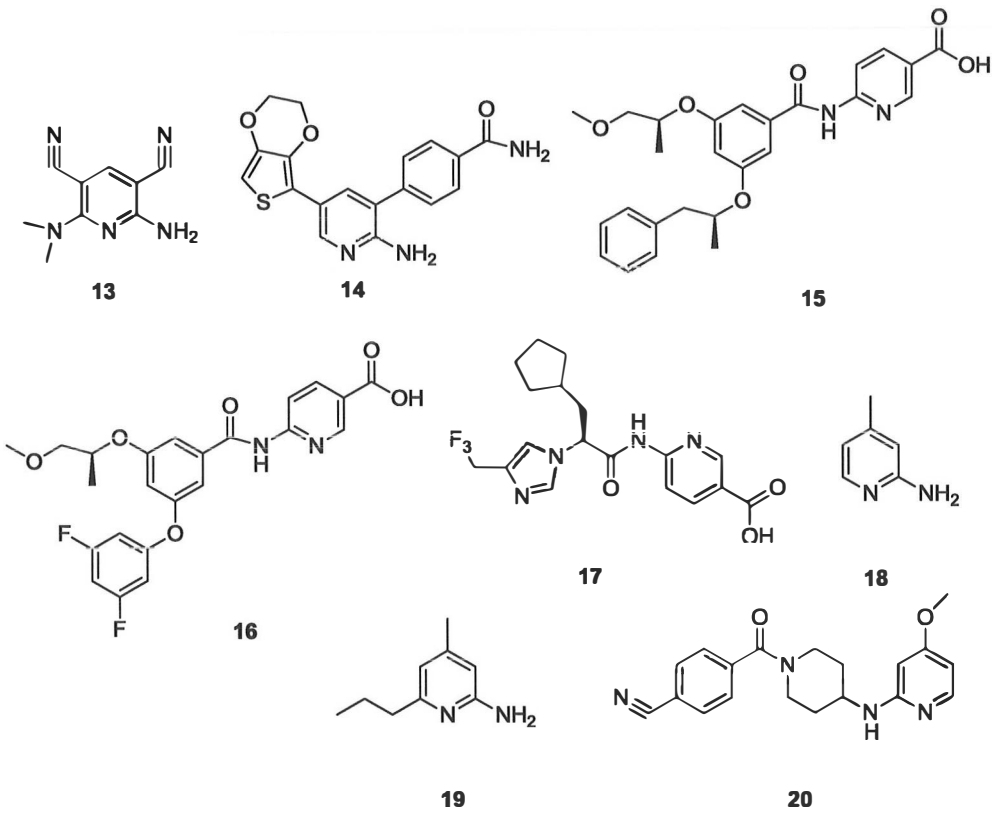

Figure 3. Biologically active compounds with 2-AP moiety.

1.2 3-Aminopyridine and its derivatives

3-aminopyridine (3-AP) is used as an intermediate in chemical syntheses.[1] A few pharmaceutically important compounds with 3-AP moiety can be found in the literature. In the following paragraphs cytostatic triapine and the 3-AP riboses used as anti-infective agents against *Haemophilus influenza*, are introduced.

Triapine (3-aminopyridine-2-carboxaldehyde thiosemicarbazone, **21**) is a ribonucleotide reductase inhibitor and a promising anticancer compound.[66,67] It binds iron, which is essential for cell proliferation as a part of ribonucleotide reductase, a rate-limiting enzyme in DNA synthesis.[68] The therapeutic efficacy of a single agent triapine in phase I and II clinical trials[69-73] as well as in combination therapy with gemcitabine[74-76], with fludarabine[77], with doxorubicin[78], and with cytarabine[79,80] against a variety of different cancer types has been modest. However, combination therapy with Cisplatin and radiation

against cervical cancer[81], currently in phase II clinical trials[82], has shown higher potency. The low cytotoxic activity of triapine may be induced by drug efflux via the multidrug resistance protein.[83] Consequently, a terminally dimethylated derivative of triapine (KP1719, **22**) has been synthesized and tested, showing higher cytotoxicity.[84]

Haemophilus influenza (Hi) is a human specific Gram-negative bacterium. Six encapsulated strains are known, of which type b (Hib) is the most virulent.[85] Diseases caused by Hib include meningitis, epiglottitis, and sepsis[85], as well as osteitis, otitis media, cellulitis, pericarditis, and pneumonia.[86] Non-encapsulated (non-typeable) strains of Hi cause local inflammations in the upper and lower respiratory tract.[85] Nicotinamide adenine dinucleotide (NAD^+) is an essential extracellular growth factor for Hi, which is not able to synthesize and recycle NAD^+.[87] Consequently, two Hi growth inhibitors have been developed based on the inhibition of NAD^+ utilization (**23**, **24**).[88] The structures of the ribonucleotide reductase inhibitors **21** and **22**, as well as of the Hi growth inhibitors **23** and **24**, are shown in Figure 4.

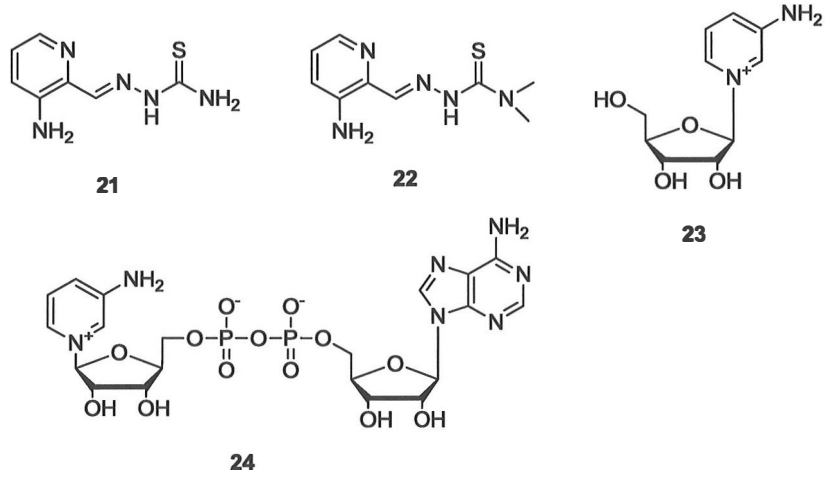

Figure 4. Ribonucleotide reductase inhibitors **21** and **22**, and Hi growth inhibitors **23** and **24**.

1.3 4-Aminopyridine and its derivatives

Two main uses of 4-aminopyridine (4-AP, **25**) are discussed in the following paragraphs, namely its use as a bird repellant (Avitrol) and as a medication for the symptomatic treatment of multiple sclerosis (MS) (Dalfampridine). Additionally, other experimental studies of the use of 4-AP to treat neurological disorders, and a selection of biologically evaluated 4-AP derivatives, are introduced.

Avitrol was first registered in 1972 as an avicide and it is currently used as a bait formulation against certain bird species, including pigeons, sparrows, and blackbirds.[89] It can be considered as a "behavior repellent". Some members of the flock are exposed to the avicide, which manifests as agitation, hyperactivity, and distress calls before the fatal outcome. This is thought to frighten the other members of the flock, leading to an avoidance behavior towards the site of the event.[90] Before the use of Avitrol, the birds are trained to feed at a specific site by pre-baiting with non-toxic baits in order to localize the "emotional shock" of the survivors.[91]

MS is estimated to affect over a million people globally[92] with large geographic prevalence differences.[93] It is primarily an inflammatory disorder of the brain and spinal cord, causing damage to myelin and axons. Both environmental and genetic factors trigger the disease; however, full disease mechanisms remain to be resolved. Many of the symptoms are non-specific, including tremor, cognitive impairment, and stiffness. Perhaps the most characteristic manifestations of MS are Lhermitte's symptom (an electrical sensation running down the spine or a thump triggered by neck flexion) and the Uhthoff phenomenon (symptoms worsen when the core body temperature increases, e.g., after a hot bath).[94]

Dalfampridine (Ampyra) was approved by the U.S. Food and Drug Administration (FDA) for the treatment of MS on January 22nd 2010.[95] It acts by blocking the potassium channels in degenerated axons leading to promotion of axonal conduction in the CNS.[96] Around 40 % of MS patients are responding to the symptomatic treatment of ambulatory disability (i.e., improving motor functions) with a dose of 10 mg twice daily[97,98], and currently patients are being recruited to determine factors that will predict a response.[99] 4-AP has a narrow therapeutic index and therefore its formulation must enable slow and constant release of the pharmaceutical in order to avoid plasma concentrations above 100 ng/mL.[100] Adverse effects of dalfampridine are estimated to be acceptable up to a 20 mg twice daily dose[101]. However, overdosing caused by formulation errors has led to severe, even lethal, complications.[102,103] Recently, 4-aminopyridine-3-methanol (**26**) has in an animal model shown higher potency in the treatment of MS compared to 4-AP[104], although safety remains to be evaluated.

The use of 4-AP in the treatment of spinal cord injury (SCI) has been disappointing.[105] Namely, it has been estimated that a concentration 100 times greater[106] than that which is acceptable due to adverse effects[107] would be beneficial. Moreover, low tolerable doses have limited the use of 4-AP in animal models of Parkinson's disease[108] as well as patients with Lambert-Eaton myasthenic syndrome (LEMS) (an autoimmune disease in which neuromuscular weakness is caused by impaired acetylcholine release. Around 60 % of patients also have small-cell lung cancer (SCLC).).[109] Therefore, derivatives such as **26**[110] and carbamates (**27**)[107,111] have been synthesized and shown to have a higher efficacy in the treatment of SCI. In addition, the 4-AP derivative **28** has shown very high potency in the animal model of Alzheimer's disease, whereas a 100-fold less potent derivative **29** has the advantage of being

considerably less toxic (LD_{50} 87 versus > 4215 μmol/kg, respectively).[112] 4-AP has also shown activity against other neurological disorders, such as myasthenia gravis (MG)[113] (skeletal muscle weakness caused by autoimmune attack against acetylcholine receptors (AChR) or non-AChR components of the postsynaptic muscle endplate)[114] and spinocerebellar ataxia type 1 (SCA1)[115] (an inherited lethal disease in which motor coordination is lost due to the loss of Purkinje cells in the cerebellar cortex in response to a mutant protein[116]). The outward K^+ current is also related to the cell cycle in many normal and malignant cell types[117], and *in vitro* studies have revealed apoptotic activity of 4-AP in malignant astrocytoma[118] and leukemia cell lines.[119] 4-AP and its biologically active derivatives **26 – 29** are described in Figure 5.

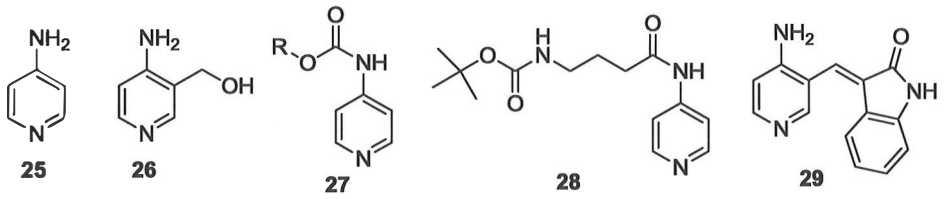

Figure 5. 4-AP and its biologically active derivatives. In **27** R = Me, Et, or *t*-Bu.

1.4 Bile acids

Bile acids (BAs) have a wide variety of biological functions in the human body. Probably their most well-known function is the digestion and absorption enhancement of dietary lipids in the intestinal tract.[120] A relatively new finding is their function as signaling molecules[121] that interact with, for example, FXR[122-124] and TGR5[125,126] receptors as well as with muscarinic receptors.[127-130]

Primary bile acids in humans, cholic acid (CA) and chenodeoxycholic acid (CDCA) are steroidal compounds synthesized in the liver from cholesterol via neutral or acidic pathways. The neutral pathway produces BAs only in the liver, whereas the enzymes needed for the initial steps in the acidic pathway are present in many tissues. The intermediates produced are finalized in the liver.[120] Interestingly, all of the enzymes needed for synthesizing CDCA via the 24(*S*)-hydroxycholesterol pathway have recently been identified in the brain.[131] After biosynthesis from cholesterol, C_{24} bile acids are conjugated mainly with glycine or taurine via *N*-acyl amidation (Scheme 3). Other recognized conjugations are sulfation or ester glucuronidation at C-24, ethereal conjugation at C-3, and *N*-acetylglucosamination at C-7. Bile acids are excreted to the gallbladder only in conjugated forms in order to avoid precipitation.[132] In the colon, the primary bile acids are exposed to the microbial flora, which is able to dehydroxylate C-7, forming the secondary bile acids deoxycholic acid (DCA) and lithocholic acid (LCA).[133] From the small intestine, over 95 % of bile acids are re-absorbed and re-circulated to the liver, undergoing cycling called

enterohepatic circulation.[134] Recent reviews provide a more comprehensive examination of this subject.[120,134,135] The general structure of C_{24} BAs, numbering and ring symbols, as well as structures of glycine and taurine are presented in Scheme 3. A selection of mammalian natural C_{24} bile acids is listed in Table 1.

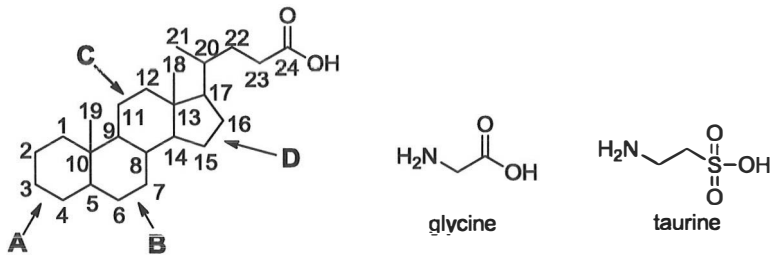

Scheme 3. Structure and numbering of the C_{24} bile acids combined with the structures of glycine and taurine, with which the BAs are mostly conjugated in the body.

Table 1. A selection of C_{24} BAs naturally occurring in mammals.

Trivial name	A/B RJ, A ring substituents	B ring substituents	C & D ring substituents	Other substituents
Cholic	5β,3αOH	7αOH	12αOH	None
Allocholic	5α,3αOH	7αOH	12αOH	None
Deoxycholic	5β,3αOH	None	12αOH	None
Allodeoxycholic	5α,3αOH	None	12αOH	None
Chenodeoxycholic	5β,3αOH	7αOH	None	None
Ursocholic	5β,3αOH	7βOH	12αOH	None
Ursodeoxycholic	5β,3αOH	7βOH	None	None
Lithocholic	5β,3αOH	None	None	None
(none proposed)	5β,3αOH	None	15αOH	None
Lagodeoxycholic	5β,3αOH	None	12βOH	None
α-Muricholic	5β,3αOH	6βOH,7αOH	None	None
β-Muricholic	5β,3αOH	6βOH,7βOH	None	None
ω-Muricholic	5β,3αOH	6αOH,7βOH	None	None
Murideoxycholic	5β,3αOH	6βOH	None	None
Hyocholic	5β,3αOH	6αOH,7αOH	None	None
Hyodeoxycholic	5β,3αOH	6αOH	None	None
Vulpecholic	5β,3αOH,1αOH	7αOH	None	None

(none proposed)	5β,3αOH,1βOH	7αOH	None	None
(none proposed)	5β,3αOH	7-oxo	None	None
(none proposed)	5β,3αOH	7-oxo	12αOH	None
(none proposed)	5β,3αOH	7-oxo	None	None (Δ^{22})
(none proposed)	5β,3αOH	7βOH	None	None (Δ^{22})
(none proposed)	5β,3αOH	7αOH	12αOH	23-(R)-OH
Phocaecholic	5β,3αOH	7αOH	None	23-(R)-OH
Bitocholic	5β,3αOH	None	12αOH	23-(R)-OH
Isolithocholic	5β,3βOH	None	None	None
Isodeoxycholic	5β,3βOH	None	12αOH	None
Isochenodeoxycholic	5β,3βOH	7αOH	None	None
Isoursodeoxycholic	5β,3βOH	7βOH	None	None
Isocholic	5β,3βOH	7αOH	12αOH	None
Allochenodeoxycholic	5α,3αOH	7αOH	None	None
Alloavicholic	5α,3αOH	7αOH	16αOH	None
(none proposed)	5β,3αOH	7αOH	12oxo	None
Cygnocholic	5β,3αOH	7αOH	15αOH	None
Avicholic	5β,3αOH	7αOH	16αOH	None
Avideoxycholic	5β,3αOH	None	16αOH	None
(none proposed)	5β,3αOH	7αOH	12αOH,16αOH	None
(none proposed)	5β,3αOH	None	12αOH,16αOH	None
(none proposed)	5β,1βOH,3αOH	7αOH	None	None
(none proposed)	5β,4βOH,3αOH	7αOH	None	None
(none proposed)	5βOH,3αOH	7αOH	None	None
(none proposed)	5β,3αOH	7αOH	12αOH	None (Δ^{22})
Haemulcholic	5β,3αOH	7αOH	None	22-(S)-OH

Abbreviations: A/B RJ, A/B ring juncture. Modified from reference 133.

Ursodeoxycholic acid (UDCA, ursodiol) has been studied extensively to be exploited in treating a variety of pathological conditions. Other bile acids have not revealed significant medicinal potency and they are not discussed in this section. However, as additives in pharmaceutical preparations, different bile salts are permeation enhancers through BBB[136], nasal mucosa[137], and buccal mucosa.[138]

UDCA was approved by the FDA in 1987 for the treatment of gallstones[139], and in 1997 for the treatment of primary biliary cirrhosis (PBC)[140], for which it is the only pharmaceutical available.[141] The efficacy of UDCA in gallstone

(cholelithiasis) dissolution therapy is limited, since it only applies to cholesterol cholelithiasis with small size, and also because the risk of recurrence of gallstones after the treatment is high.[142] No response has been observed with patients with biliary colic awaiting cholecystectomy[143], however, after bariatric surgery, when the risk of gallstone formation is increased, UDCA has been shown to be beneficial.[144] PBC is a progressive autoimmune disease that eventually leads to liver failure due to the destruction of the intrahepatic bile ducts. The cause of the autoimmune reaction directed to ubiquitous mitochondrial autoantigens leading to pathological changes only in the biliary epithelial cells, is not fully understood.[145] UDCA, however, is reported to delay the progression of early-stage PBC at a dose of 12 to 15 mg/kg/day[145]. It is currently the standard treatment for patients with PBC, with an estimated response rate of 60 - 65 %[146], although the efficacy of the treatment is still controversial.[147]

Primary sclerosing cholangitis (PSC) is a chronic cholestatic liver disease. In the majority of cases inflammatory bowel disease (IBD) precedes the development of PSC.[148] Unlike PBC, which primarily affects middle-aged women[145], most of the PSC patients are young or middle-aged men.[148] The benefits of low-dose (8 - 13 mg/kg/day) UDCA treatment of PSC have been modest[149], whereas the clinical efficacy of UDCA in 30 mg/kg/day doses has been reported to be more beneficial.[150] However, recent studies of the high-dose treatment of PSC have shown serious adverse effects[151], as well as an increased risk for colorectal neoplasia.[152] It has been suggested that, with high doses, the unabsorbed UDCA enters the colon where it is modified by bacterial flora to hepatotoxic lithocholic acid (LCA), which then causes the adverse effects.[151]

Colorectal cancer (CRC) is the second most common cancer type in women and the third most common in men[153], causing an increasing number of deaths worldwide[153,154], although mortality rates differ greatly between countries.[155] CRC is generally classified as a single cancer type[156], however, since proximal and distal (divided by splenic flexure) parts of the colon have distinct physiology, molecular biology, and embryological origin, CRC should be differentiated into these subtypes.[157] Furthermore, the clinical outcome of CRC in these subtypes is different.[157] Based on this background, it is not surprising that controversial results have been obtained in studies using UDCA in CRC chemoprevention.[158] In addition, the effectiveness of UDCA in chemoprevention of colorectal adenoma progression has been shown to be gender-dependent.[159] Taken together, UDCA may have a positive future in the chemoprevention of well-specified types of CRC.

UDCA and its taurine (TUDCA) and glycine (GUDCA) conjugates have shown activity against many neurological dysfunctions. TUDCA is able to cross the BBB and accumulate in the brain[160], and has shown neuroprotection in Huntington's disease (HD)[160], Alzheimer's disease[161,162], and Parkinson's disease.[163] Furthermore, UDCA has shown neuroprotection against injuries caused by Cisplatin[164] and GUDCA against bilirubin-induced injuries.[165] UDCA has also been used in the treatment of autosomal recessive ataxia.[166]

2 POLYMORPHISM AND ITS SIGNIFICANCE IN PHARMACOLOGY

2.1 Introduction

Polymorphism in chemistry is defined as the ability of a molecule or element to adopt at least two different crystal arrangements in the solid state, while having a single liquid and vapor state.[167] Crystal arrangement in this definition refers to the repeating chemical units over a large volume (compared to the single chemical unit) described by a set of three-dimensional translationally periodic symmetry operations.[168] As a concept, polymorphism was introduced to the scientific literature in 1788 by Klaproth, when calcium carbonate was observed to crystallize as calcite, vaterite, and aragonite.[169] In 1832, Wöhler and Liebig published the first paper describing polymorphism of an organic compound, benzamide. To address the complexity of polymorphism, it took 175 years to identify the metastable polymorph from the original publication.[170,171] Furthermore, the structure of the third polymorph of benzamide was not published until a few years ago[172], and efforts to obtain *in silico*-predicted polymorphs are still in progress.[173] In this section, different types of polymorphism are defined, followed by an introduction of one-component crystal growth in solution. Ritonavir as a pharmaceutical example of polymorphism is also discussed, as are the principal analytical methods in the research of polymorphism.

Polymorphism of elements is termed "allotropism". Well known examples are allotropes of carbon, such as graphite, diamond, fullerenes, and carbon nanotubes. Molecular polymorphism can be characterized as "packing" or "conformational" polymorphism, related to the structural differences. From a thermodynamic point of view, polymorphs can be characterized as monotropes – when only one polymorph is stable at all temperatures below the melting point – or as enantiotropes – when polymorphs are stable in different temperature and pressure ranges.[174] From the crystallization point of view, concomitant or sequential polymorphism can be classified, i.e. polymorphs can

be crystallized simultaneously or they can only be crystallized at different temperatures, respectively.[175] "Tautomeric polymorphism" refers to species that interconvert rapidly in solution or melt, whereas the term "desmotropy" is used to describe slowly interconverting species.[176] In addition, the concept of polymorphism encompasses multicomponent systems, where liquid or solid molecule(s) are incorporated into a crystal lattice.[177] Solvates are crystalline solids, in which solvent molecules are present in the crystal structure. When the solvent molecule is water, the solvates are called hydrates.[178] If the definition according to which polymorphs have identical elemental composition is adhere to, solvates and hydrates are less prone to polymorphism than single component compounds.[179] Solvates and hydrates are also occasionally called "pseudopolymorphs", although this term is misleading and should be avoided.[180] Co-crystals are composed of two or more neutral molecular species that are solids at ambient conditions[181] and, as in the case of solvates and hydrates, they appear to have a low tendency to form polymorphs.[182] Unfortunately, the term pseudopolymorphism has recently been adopted in the field of co-crystals, where it has been used to describe crystals with a different ratio of the components.[183] Because salts are excluded from the definition of co-crystals, their distinct crystal modifications are simply named polymorphs (e.g., two polymorphs of the antibacterial agent acrinol (**30**, Figure 6) are composed of 2-ethoxy-6,9-diaminoacridine and lactate).[184] It should be noted that in the field of biology the term "crystal polymorphism" is used more widely to include hydrates with different stoichiometries.[174,185] In physical pharmacy, for one, polymorphism refers to all kinds of solid formulations of active pharmaceutical ingredients (APIs), including amorphous forms.[186]

2.2 Crystal growth in solution

For polymorphic systems, crystallization from a solution is essentially determined by a combination of thermodynamic and kinetic factors[187], as well as fluid dynamics.[188] The first step in the formation of crystalline material from solution is nucleation, which is defined as a process where atoms or molecules rearrange into a cluster large enough to grow irreversibly to the macroscopic scale.[189] The driving force for nucleation is supersaturation, which can be expressed for non-ionic species with the following equations,

$$\Delta\mu = \mu_s - \mu_c \quad (1)$$

$$\Delta\mu = kT\ln S \quad (2)$$

$$S = C/C_e \quad (3)$$

where $\Delta\mu$ is the chemical potential in Joules, subscripts s and c are solution and crystal phases, respectively, k is the Boltzmann constant, T is the absolute temperature, S is the saturation ratio, and C/C_e is the actual concentration divided by the solubility. When $\Delta\mu$ is positive, the solution is supersaturated

and the solutes are prone to form clusters.[190] It should be noted that the use of antisolvents in crystallization creates local supersaturation areas due to fluid dynamics.[191] The work (W in Joules) needed to form a cluster with n molecules for homogeneous nucleation (HON) is,

$$W_{(n)} = -nkT\ln S + \Phi_{(n)} \quad (4)$$

where Φ (in Joules) is the total surface energy of the cluster (solid-solvent interface). If $\Phi = 0$, then Eq. 4 simply describes the work for precipitation. In the case of heterogeneous nucleation (HEN), i.e., nucleation induced by the solid substrate (e.g., dust or a scratch in the flask), the nucleation barrier is substantially lower in comparison to that of HON. Obviously, the surface energy term in Eq. 4 becomes more complicated, since both the solid-solvent and the solid-solid interfaces have to be considered. An important practical consideration in crystallization experiments is the kinetic metastable zone of supersaturation (above solubility, but below critical supersaturation), in which crystallization is arrested for a certain time.[190] This permits the four crystal growth processes of atoms or molecules: transport through solution, attachment to the surface, movement on the surface, and attachment to edges and kinks.[189]

2.3 Ritonavir – an example illustrating drug polymorphism

Drug polymorphism has received extensive attention since the late 1960s[192], when different polymorphs of chloramphenicol palmitate (**31**), a taste-masking prodrug of the antibiotic chloramphenicol, were observed to have distinct bioavailabilities.[193] Drug molecules ordinarily have several functional groups in order to interact with the therapeutic target and a multitude of hydrogen bonding possibilities. Therefore polymorphs are known for most of the pharmaceutical compounds.[194] Today, solid form screening is a regulatory requirement for new pharmaceuticals.[195]

In the mid-1990s, ritonavir (ABT-538, **32**) was shown to be an effective human immunodeficiency virus (HIV) protease inhibitor with high oral bioavailability.[196] Consequently, semisolid capsule and liquid formulations (Norvir®) came into the market in 1998 by Abbott.[197] Because of its dose-related adverse effects, it is now used in low doses as a pharmacokinetic enhancer with other protease inhibitors.[198,199] During the drug development process of ritonavir, comprehensive polymorph screening was conducted, yielding only one crystal modification.[200] Both of its formulations were derived from ethanol/water-based solutions and, at that time, no crystal form control for solutions was required by the International Committee on Harmonization (ICH) guidelines.[201] After 240 semisolid patches were produced in 1998[201], the dissolution tests started to fail and a thermodynamically more stable and much less soluble form II was identified.[197] The manufacture of this drug was

terminated immediately[197], and the financial losses for Abbott in Norvir sales in 1998 are estimated to be 250 million USD.[202]

Several examples illustrate the disappearance of the previously produced metastable polymorph from the market after the discovery of a more stable form.[203] This was exemplified in the Abbot's Italian factory, where the production of ritonavir form I was successfully continued until a visiting scientist exposed the existence of form II.[197] Polymorphs of ritonavir were soon characterized to show conformational polymorphism around the carbamate linkage (Figure 7). The *cis*-conformation (form II) possesses a more stable packing arrangement, but its nucleation is energetically unfavored.[201] A degradation product, cyclic carbamate (**33**), was identified to induce a heterogeneous nucleation resulting in form II.[200] As a consequence of these developments, reformulated, soft-gelatin-derived capsules of ritonavir were approved by the FDA in June 1999.[204] In addition, the extended high-throughput crystallization experiments conducted for ritonavir revealed a third polymorph along with hydrate and formamide solvate forms.[205] The structures of acrinol (**30**), chloramphenicol palmitate (**31**), ritonavir (**32**), and an impurity (**33**) inducing crystallization of form II of ritonavir are presented in Figure 6.

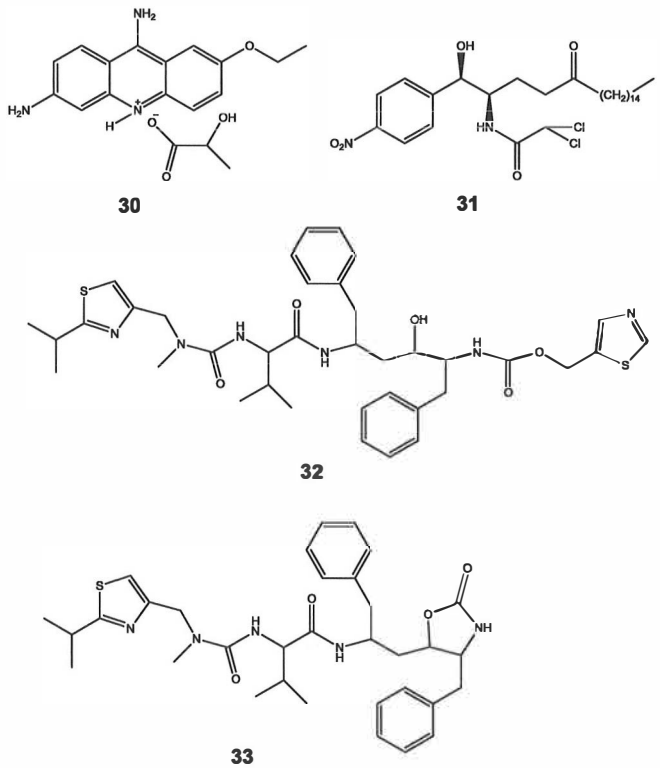

Figure 6. Examples of polymorphic pharmaceutical compounds and an impurity **33** inducing crystallization of form II of **32**.

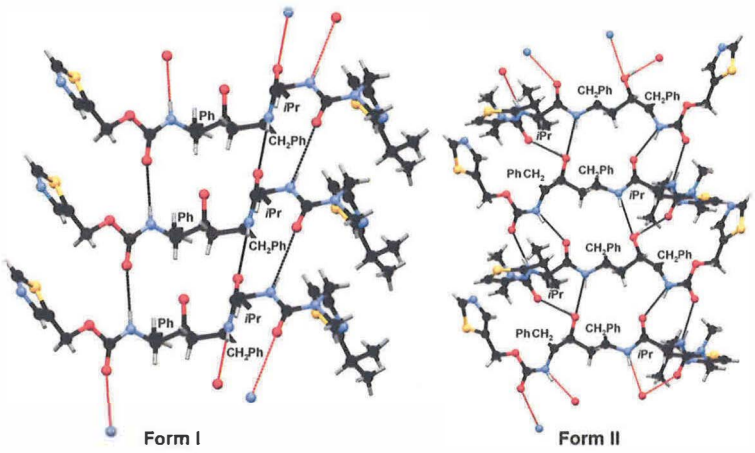

Figure 7. Packing pattern of ritonavir (**32**) forms I (left) and II (right) with hydrogen bonding network shown with dashed lines. Reproduced by permission of The Royal Society of Chemistry.[202]

2.4 Analytical methods in crystal form characterization

A variety of techniques is used in the research of solid state forms of pharmaceuticals, including solid state nuclear magnetic resonance (SS-NMR), infrared (IR) and Raman spectroscopies, single crystal and powder X-ray diffraction (XRD), as well as thermogravimetry (TG) and differential scanning calorimetry (DSC). Unambiguous characterization of the studied crystal forms usually requires a combination of these methods.[206]

NMR spectroscopy gives detailed information about the local environment of the studied nucleus. In the solid state, no long range order is required (whereas this is a requirement of single crystal X-ray diffraction, for example), enabling the studies of amorphous solids alongside crystalline materials. Heterogeneous systems can also be studied and quantified to less than 1 % of the total sample. The main disadvantages include the relatively large sample amount needed, and in some cases, the long experimental times.[207] However, since SS-NMR is a non-destructive technique[208], the sample can be reused after the measurement. In general, polymorphs are easily distinguished by visual inspection as shown in Figure 8, which presents the SS-NMR spectra of two polymorphs of carbamazepine.[209]

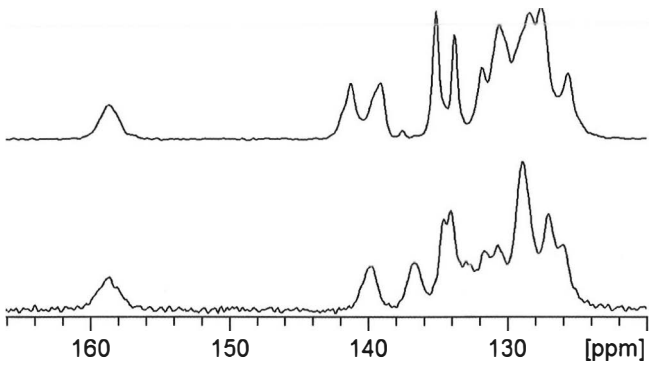

Figure 8. ^{13}C SS-NMR spectra of P-monoclinic (bottom) and trigonal (top) polymorphs of carbamazepine. According to results published by Harris and co-workers[209], the polymorphs were isolated and the above spectra then measured in our laboratory.

IR and Raman spectroscopies are complementary techniques based on transitions between quantized molecular vibrational energy states.[210] The IR spectrum is produced by the infrared region of the electromagnetic radiation. When the frequency of the radiation exactly matches the frequency of the bond vibration (resonance), energy is absorbed. The requirement for IR activity is a change in the dipole moment of the bond and therefore only heteronuclear diatomic bonds and homonuclear bonds with uneven electron distribution in larger molecules give a signal in the IR spectrum. On the other hand, Raman activity is based on molecular polarizability, i.e., a change in the size or shape of the electron distribution, thus rendering the dipole moment unnecessary. A high energy photon produced by laser irradiation is absorbed and consequently released, leaving the bond in question at a higher vibrational level.[211] Because of the very small quantity of sample needed for Raman spectroscopy, the technique is often used for a primary analysis of different crystal forms in high-throughput (HT) crystallization experiments.[212]

Single crystal XRD is considered the golden standard in structural elucidation.[213] It is based on translational symmetry and therefore gives information only about crystalline material.[214] The X-rays interact with electrons, and from the resulting reflections the unit cell and heavy atom positions can be calculated, permitting the elucidation of the 3-dimensional structure(s) of the molecule(s).[215] Unfortunately, the electron-poor hydrogen atoms are often misplaced in single-crystal X-ray structures[216], especially if hydrogen bonding is involved.[217] However, the accurate positions of hydrogen atoms can be obtained by neutron diffraction[217], or combining data from X-ray and SS-NMR experiments via computational methods.[v] Powder XRD, on the other hand, also gives information about the amorphous samples (broad maxima in diffraction patterns called "X-ray amorphous halos"), and it is used mainly for solid form identification.[218]

TG measures mass properties of the sample, from which the decomposition temperature(s) can be obtained. From DSC data, the heat capacity, phase changes, and progression of possible reaction(s) can be obtained.[219] Several types of DSC and TG curves can be obtained for polymorphic systems. Based on reference 220, six different cases are presented in the following:

1) An exothermic transition for a monotrophic system or an endothermic transition for an enantiotrophic system before melting of the high-melting form in the DSC scan is seen, corresponding to a solid to solid transition. No mass loss is observed in the TG scan for the lower temperature transition.
2) Two exothermic transitions are seen in the DSC scan, while only one decomposition is seen in the TG. This may correspond to the crystallization of the lower-melting form from the melt to either a monotropic or an enantiotropic higher-melting form, although a possible isomerization should be ruled out by other analytical methods.
3) No conversions are observed in DSC scans, indicating that each crystal form has its own melting point.
4) An endothermic peak in DSC is related to mass loss in TG before the decomposition temperature corresponding to hydrate/solvate forms.
5) When an exotherm is seen during or after the melting of the hydrate/solvate, a solvent free form has crystallized from the melt.
6) Solvates/hydrates with the same chemical composition but different polymorphic form may exist. Examples of the DSC and TG curves of two dihydrate forms of L-706,000-001T, an antiarrhythmic compound, are shown in Figure 9.[221]

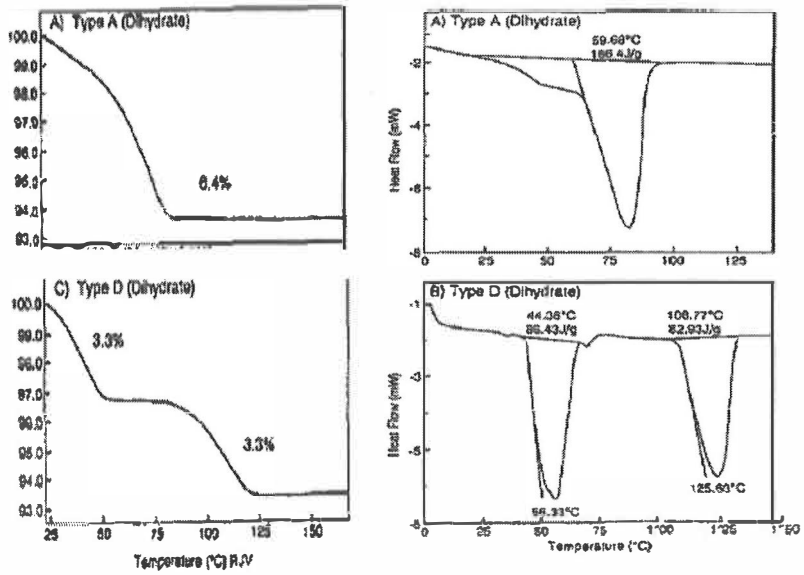

Figure 9. TG (left) and DSC (right) scans of two dihydrate polymorphs of L-706,000-001T. Reproduced by permission of IOP Publishing Limited.[221]

3 EXPERIMENTAL

3.1 Aim of this work

The main objective of this work was to study different crystal forms of bile acid derivatives consisting of bile acids with varying amounts of hydroxyl groups and a selection of small molecules combined via an amide linkage. Information about the solid state structures of molecules with potential pharmaceutical activity is important, since – as pointed out in the review of the literature part of this thesis – different crystal forms may possess different chemical, physical, and pharmaceutical properties.

Isomeric aminopyridines have shown a wide variety of biological activities. Their conjugation with bile acids may be beneficial for bioavailability, targeting, and/or activity. Indeed, the latter was proven for chenodeoxycholic and ursodeoxycholic conjugates of 4-aminopyridine, whose activities were tested in rat brain samples (unpublished results). The bile acid-aminoalkyl conjugates, on the other hand, probably do not possess direct pharmacological activities, but rather have the potential to act as low molecular weight gelators and consequently to serve as a formulation media for active pharmaceutical ingredients. Their ability to form gels in certain organic solvents has recently been proved in our laboratory.[222] Obviously, the solid state forms of these conjugates may have an influence for the gel formation.

An additional objective of this work was to evaluate the power of the GIPAW computational method as a bridge between the experimental single crystal XRD and SS-NMR data. Whereas positions of heavy atoms are accurately determined by single crystal XRD data, the positions of the hydrogen atoms cannot be determined from their diffraction. The influence of optimizing the hydrogen positions of single crystal XRD structure on the SS-NMR data was evaluated in papers IV and V.

3.2 Preparation of the target molecules

Lithocholyl-*N*-(2-aminoethyl)amide (**36**) was synthesized as described in Scheme 4. Excess 1,2-diaminoethane was used in the synthesis and crystalline **36** was obtained by precipitation from water followed by recrystallization from acetonitrile (AcCN).[I]

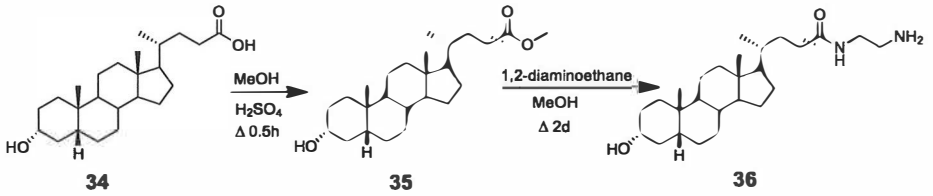

Scheme 4. The synthesis of lithocholyl-*N*-(2-aminoethyl)amide (**36**).

Isomeric aminopyridines have shown a wide variety of biological activities. The isomeric aminopyridine derivatives of lithocholic acid were synthesized in a single-mode microwave (MW) reactor without solvent. Ten to twenty equivalents of aminopyridines were used and the reaction temperature varied between 230 and 250 °C (Scheme 5). Unreacted reagents were washed out with an aqueous alkaline solution and aminopyridine conjugates **37 – 39** were purified by recrystallization from AcCN.[II] A large excess of aminopyridines was needed to avoid formation of lithocholate ester as a by-product, evidenced when three equivalents of 8-aminoquinoline were used in equal experimental conditions (unpublished results).

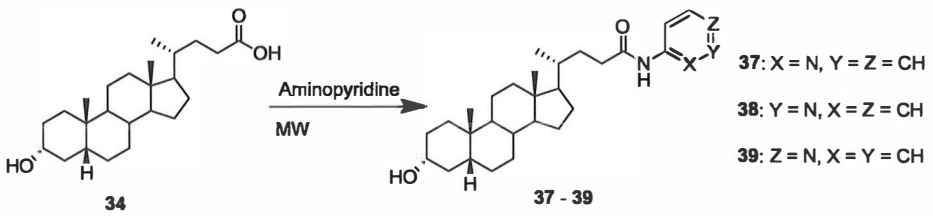

Scheme 5. The synthesis of isomeric aminopyridine derivatives of lithocholic acid (**37 – 39**).

Bile acid 4-aminopyridine conjugates **50 – 54** were synthesized as described in Scheme 6. The TEA salt was filtered off and the solvent evaporated under reduced pressure. The unreacted 4-AP and BA were removed by washing with aqueous bicarbonate solution followed by refluxing in AcCN, and the resulting white powder was dried in vacuum.[III]

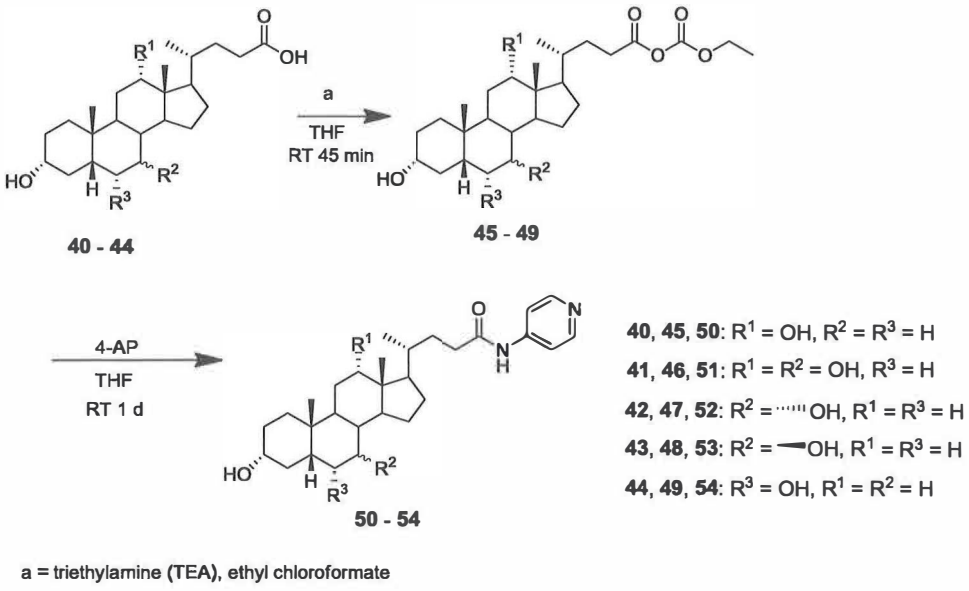

Scheme 6. The synthesis of bile acid 4-aminopyridine conjugates **50 - 54**.

Solid state NMR experiments for isocytosine were conducted using fully ^{15}N-labeled isocytosine, whose synthesis is described in Scheme 7. The reaction mixture was poured onto ice and the pH of the resulting solution was adjusted to 9 before column chromatography. Compound **57** was recrystallized from water.[IV]

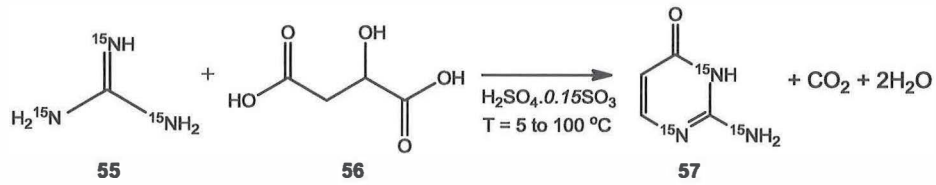

Scheme 7. The synthesis of fully ^{15}N labeled isocytosine **57**.

2-Alkanamido-6-[1*H*]-pyridones **61** and **62** were synthesized by boiling 6-amino-2-[1*H*]-pyridone (**58**) with acid chlorides **59** and **60** in pyridine for 6 hours (Scheme 8). After washing with water and cold ethanol, the pure products were obtained by recrystallization from ethanol.[V]

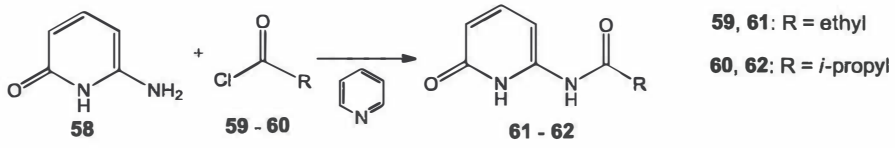

Scheme 8. The synthesis of 2-alkanamido-6-[1*H*]-pyridones **61** and **62**.

3.3 Polymorph/solvate crystallization and analysis

3.3.1 Lithocholyl-*N*-(2-aminoethyl)amide[I]

Four different solid state forms were obtained for lithocholyl-*N*-(2-aminoethyl)amide **36**, of which three had solvent molecule(s) incorporated into the structure, namely *p*-xylene (**36b**), *iso*-propanol (**36c**), and diethyl ether (**36d**). Furthermore, **36** formed gel-like material in chlorobenzene (**36e**). All forms were obtained by dissolving **36** in boiling solvent after which the resulting solution was filtered and kept at RT. The anhydrous form of **36** (**36a**) was obtained from AcCN, THF, and 1,4-dioxane. The primary methods for analyzing the different crystal modifications of **36** were ^{13}C- and ^{15}N SS-NMR. Moreover, the anhydrous form **36a** and the *p*-xylene solvate **36b** were subjected to powder X-ray diffraction studies as well as to DMFIT simulations.

Clear differences were observed in the ^{13}C SS-NMR spectra of **36a – 36e**, as illustrated in Figure 10. In addition to the distinct chemical shifts for the carbons of the core molecule, the solvate resonances of aromatic carbons in the cases of **36b** and **36e** were visible at around 130 ppm, whereas in the cases of **36c** and **36d** the methine and the methylene carbons at around 70 ppm, respectively, were overlapping with the C3 resonances of the core molecule. The ^{13}C SS-NMR spectrum of the bulk synthetic product **36** showed several resonances for each carbon, indicating the existence of different polymorphic forms. Although no polymorphs were reported in paper I, the procedure reported in the paper for preparing and crystallizing the anhydrous form **36a** resulted in another crystal modification as a result of the second synthesis as shown in Figure 11 (unpublished results by author). This is not surprising, since usually the crystallization conditions cannot be reproduced exactly.

The powder XRD analysis further confirmed that **36a** and **36b** were different crystalline structures. The DMFIT calculations were conducted for these forms, andwere based on spinning side band (SSB) analysis of the carbonyl carbon C24. Since the principal tensor component δ_{22} is oriented close to the carbonyl bond, deshielding of δ_{22} of **36b** compared to that of **36a** reflects a longer hydrogen bond C=O···H in the former.[V] This may result from an interaction between the solvent molecule and the carbonyl oxygen or a different packing pattern of the host molecule. Results of the DMFIT simulations are depicted in Table 2.

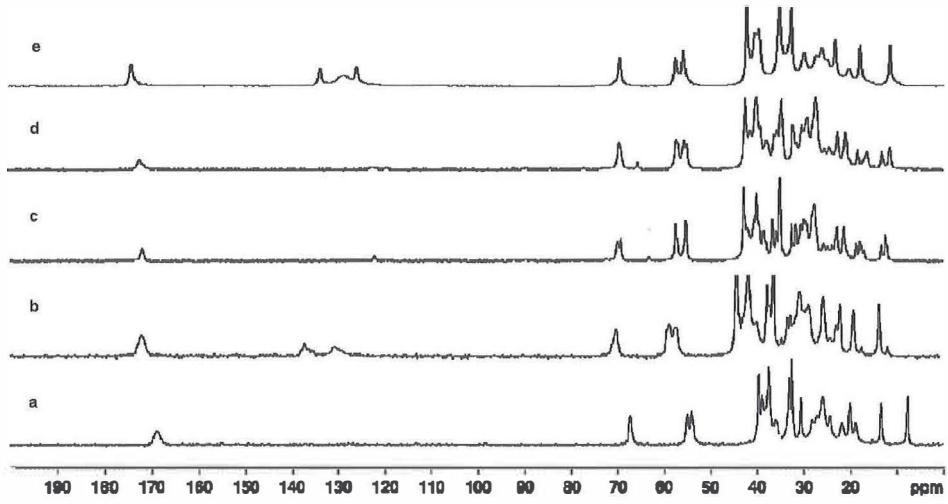

Figure 10. The ^{13}C SS-NMR spectra of different solid state forms obtained for lithocholyl-*N*-(2-aminoethyl)amide **36a – 36e** (a = anhydrous form, b = *p*-xylene solvate, c = *iso*-propanol solvate, d = diethyl ether solvate, e = chlorobenzene solvate).

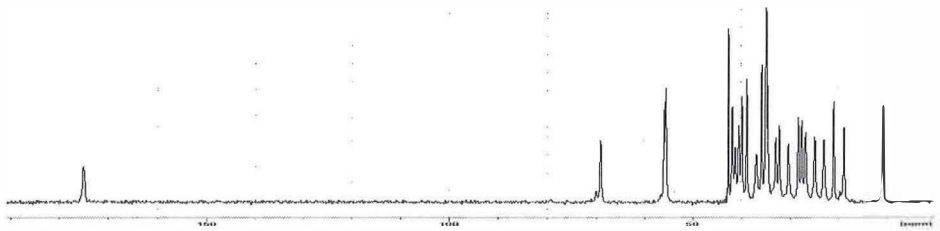

Figure 11. The ^{13}C SS-NMR spectrum of the anhydrous form **36a** obtained from the second patch (unpublished results by author).

Table 2. CSA tensor components (ppm) of the carbonyl carbon in **36a** and **36b**, assuming $\delta_{11} > \delta_{22} > \delta_{33}$, $\delta_{iso} = (\delta_{11} + \delta_{22} + \delta_{33})/3$, $\eta = (\delta_{22} - \delta_{11})/(\delta_{33} - \delta_{iso})$, CSA = δ_{33}-δ_{iso}.

Parameter	36a	36b
δ_{11}	245.4	243.2
δ_{22}	173.0	177.3
δ_{33}	88.6	94.0
η	0.90	0.85
CSA	-80.4	-77.5
δ_{iso}	169.0	171.5

3.3.2 Isomeric aminopyridine derivatives of lithocholic acid[II]

The different crystal modifications for the isomeric aminopyridine derivatives of lithocholic acid **37 – 39** were obtained from AcCN. ^{13}C SS-NMR spectroscopy was used to differentiate these forms, and their spectra are shown in Figure 12. Furthermore, the single crystal X-ray structures of **37a** and **39a**, which are shown in Figure 13, were solved. Powder XRD patterns were measured for all of the samples, and in order to confirm the possible formation of a hydrate (no solvent resonances were seen in ^{13}C SS-NMR spectra), TG analyses were conducted (Figure 14). ^{13}C SS-NMR spectra were re-measured after six months to ensure the stability of the crystal forms.

The single crystalline form of the 2-AP derivative of lithocholic acid (**37a**) was obtained by a slow crystallization from a dilute AcCN solution, whereas another form (**37b**) was crystallized quickly from a more concentrated AcCN solution. Due to the very low quantity of **37a** obtained, its SS-NMR spectrum was not measured. Differences between forms **37a** and **37b** were confirmed by comparing the simulated powder diffraction pattern of **37a** and the experimental powder XRD pattern of **37b** with each other. Based on TG analysis, these forms were anhydrous polymorphs of **37**.

From AcCN and chlorobenzene the 3-AP derivative of lithocholic acid **38** crystallized as a dihydrate (**38a**, Figure 14). However, the SS-NMR spectrum measured after six months was profoundly different, and a new anhydrous form **38b** (Figure 12) was identified.

In the case of the 4-AP derivative of lithocholic acid, slow crystallization from a dilute AcCN solution resulted in single crystals (**39a**). Another form **39b** was crystallized quickly from a more concentrated AcCN solution, whereas **39c** was obtained by a slow evaporation of AcCN into dryness. Based on TG analysis, **39a** and **39b** were anhydrous polymorphs, whereas **39c** was a hemi-trihydrate. The ^{13}C SS-NMR spectrum recorded for the sample of **39a** after one month resulted in a spectrum equivalent to that of **39c**. Due to the instability of the crystals at ambient conditions and low quantity, a ^{13}C SS-NMR spectrum was not obtained for the fresh sample of **39a**. Rietveld refinement conducted for **39b** showed conformational polymorphism in **39** (Figure 15).

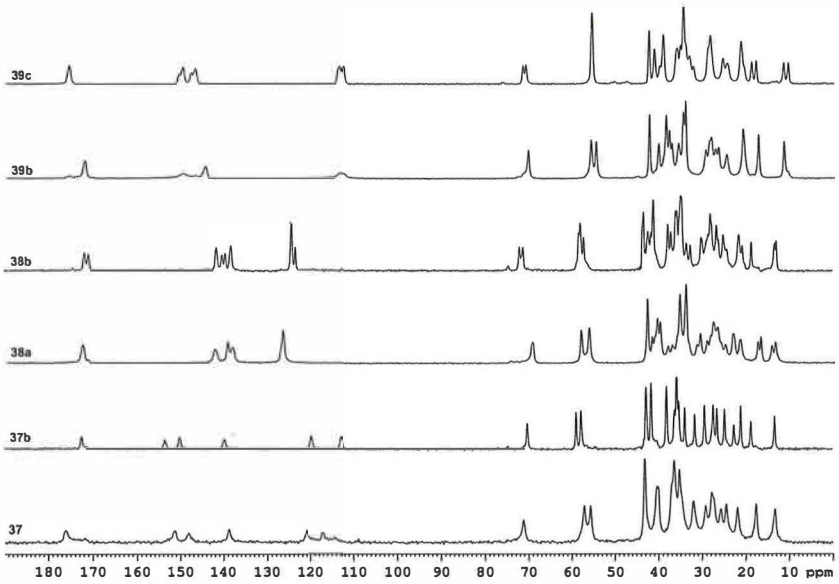

Figure 12. ^{13}C SS-NMR spectra of the different crystal modifications of the isomeric aminopyridine derivatives of lithocholic acid **37 – 39** (**37** = the bulk synthetic product of the 2-AP derivative, **37b** = the anhydrous polymorph of the 2-AP derivative, **38a** = dihydrate of the 3-AP derivative, **38b** = the anhydrous form of the 3-AP derivative, **39b** = the anhydrous polymorph of the 4-AP derivative, **39c** = the hemitrihydrate of the 4-AP derivative).

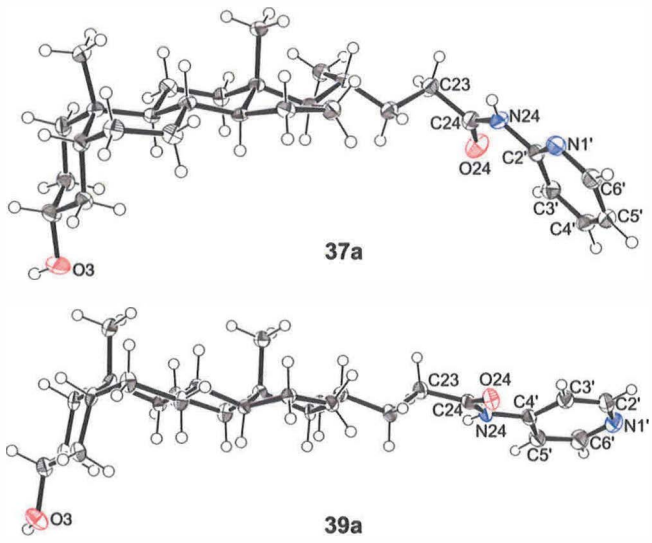

Figure 13. The single crystal X-ray structures of **37a** (lithocholyl-*N*-(2-aminopyridyl)amide) and **39a** (lithocholyl-*N*-(4-aminopyridyl)amide) with partial numbering.

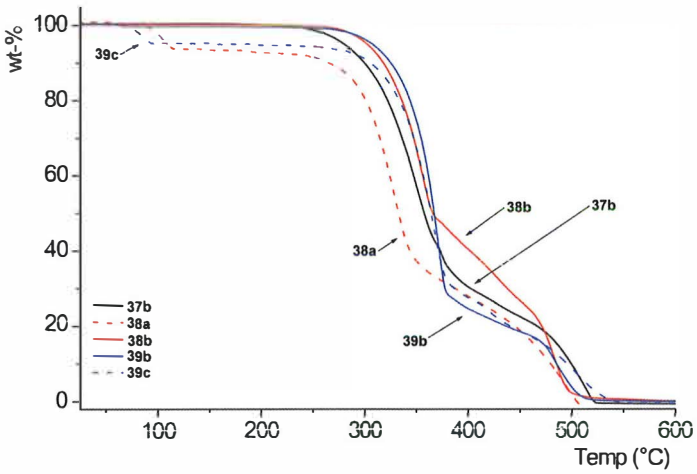

Figure 14. The TG curves of the isomeric aminopyridine derivatives of lithocholic acid **37** – **39** (**37b** = the anhydrous form of the 2-AP derivative, **38a** = dihydrate of the 3-AP derivative, **38b** = the anhydrous form of the 3-AP derivative, **39b** = the anhydrous polymorph of the 4-AP derivative, **39c** = hemitrihydrate of the 4-AP derivative).

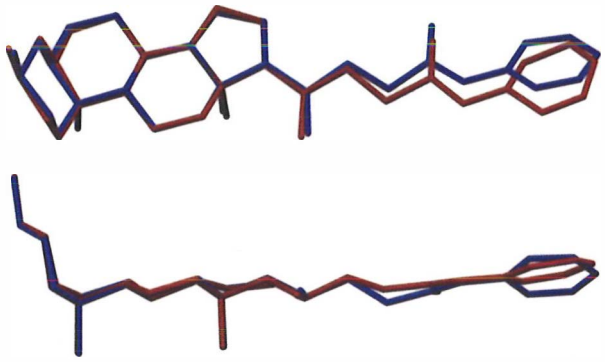

Figure 15. The molecular structures of the polymorphic forms of lithocholyl-*N*-(4-aminopyridyl)amide **39a** (blue) and **39b** (red).

3.3.3 4-Aminopyridine conjugates of bile acids containing from two to three hydroxyl groups[III]

Systematic crystallization experiments were conducted for a series of five 4-aminopyridine conjugates of bile acids other than lithocholic acid (**50** - **54**), resulting in a total of twelve different crystal modifications. In order to ensure the optimal crystallization conditions the following procedures were applied: i) "pro-solvent" (either ethanol or DMSO) was added step-by-step to the mixture if, despite ultrasonic treatment and/or heating, the compound did not dissolve,

or ii) "anti-solvent" (either water or acetone) introduced step-by-step whenever the dissolution took place instantly. Solvents/solvent mixtures from which crystallization took place are summarized in Table 3.

Table 3. A selection of solvents used to crystallize the 4-aminopyridine conjugates of bile acids containing two to three hydroxyl groups **50 - 54**. Solvent mixtures are shown in parentheses.

Compound / Main solvent	**50**	**51**[3]	**52**	**53**	**54**
Synthetic product	**50a**	**51a**	**52a**	**53**	**54**
Ethanol	**50a**[1] (2:1:2 ethanol: acetone:water)	**51d** (1:1 ethanol: acetone)	**52a** (2:1 ethanol: water)	**53a**[6] (4:3 ethanol: water)	**54**
Methanol	**50a** (4:1 methanol: water)	**51c** (2:1 methanol: water)	**52a** (2:1 methanol: water)	**53** (5:2 methanol: water)	**54**
1-Propanol	**50a** (4:1 1-propanol: water)	**51c** (1:1 1-propanol: water)	**52a** (4:5 1-propanol: water)	**53** (2:5 1-propanol: water)	**54**
2-Propanol	**50a** (4:1 2-propanol: water)	-	**52a** (1:1 2-propanol: water)	**53** (1:1 2-propanol: water)	**54** (8:1 2-propanol: DMSO)
2-Butanol	**50b**	**51c, 51e**[4] (2:1 2-butanol: water)	-	Amorphous (3:1 2-butanol: water)	**54**
Anisole	**50c**[2]	-	Amorphous	-	**54** (4:1 anisole: DMSO)
Chloroform	**50a** (6:1 chloroform: ethanol)	**51b, 51d**[4] (4:1 chloroform: ethanol)	Amorphous, chloroform in the structure	Amorphous (2:1 chloroform: ethanol)	**54** (4:1 chloroform: ethanol)
Toluene	**50a** (4:1 toluene: ethanol)	Amorphous, toluene in the structure (2:1 toluene: ethanol)	Amorphous, toluene in the structure (5:2 toluene: ethanol)	Amorphous, toluene in the structure (5:3 toluene: ethanol)	**54** (4:5 toluene: ethanol)
Acetonitrile	**50a** (2:1 acetonitrile: ethanol)	**51b** (2:1 acetonitrile: ethanol)	**52a** (2:1acetonitrile: ethanol) **52b**[5]	**53** (1:1 acetonitrile: ethanol)	**54** (1:2 acetonitrile: ethanol)

- = No clear results were obtained.

[1] In addition to solvents presented in the table, form **50a** was obtained from the following primary solvents or their mixtures: acetone, THF, 1,4-dioxane, 1:1 DMF:acetonitrile, 2:1 xylene:ethanol, and 10:1 toluene:DMSO.

[2] Obtained from 2 % w/v concentration.

[3] Gel was formed in 1,1,2,2-tetrachloroethane (2 % w/v).

[4] Different forms were obtained in a second crystallization experiment. Form **51d** was also obtained from a 50:1 $CHCl_3$:ethanol solution. Form **51e** was also crystallized from a 2:1 2-butanol:ethanol solution.

[5] Form **52b** was obtained from a saturated acetonitrile solution and its existence confirmed by solid state NMR. Despite of numerous attempts, we were not able to reproduce form **52b**, resulting in an incomplete characterization of this form.
[6] Form **53a** was also obtained from a 1:1 ethanol:acetone solution.

Preliminary screening of the samples was performed by Raman spectroscopy. The existence of different crystal forms suggested by Raman spectra was confirmed by powder XRD analysis. Since only 10 – 20 mg of the sample was used for the preliminary crystallization experiments, larger amounts were crystallized for SS-NMR analysis. The chemical and structural integrity between these patches was confirmed by ATR-FTIR spectroscopy. Moreover, thermoanalytical methods (TG and DSC) were applied on the different crystal forms and thermal properties of compounds **50** – **54** are summarized in Table 4.

Table 4. The thermal properties of compounds **50 – 54**.

	Δwt-% (TG)		Solvate[a]	Thermal transitions			Dec
	exp.	*calc.*		T_{ds} (ΔH)	T_m (ΔH)	T_g (ΔC_p)	T_d
50a	4.32	3.70	w (1)	99 (123.60) [b]	222.1 (64.83)	104.7 (0.44)	300
50b	8.65	7.33	b (½)	124 (58.73)	229.6 (45.60)	127.8 (0.18)	311
50c	4.37	7.14	as (⅓)	134 (50.41) [b]	238.5 (45.91)	127.0 (0.60)	308
51a			an		275.8 (104.96)	139.9 (0.28)	323
51b	7.03	6.92	w (2)	60 (97.02) [b]	277.5 (95.94)	140.9 (0.33)	319
51c	4.59	3.59	w (1)	101 (104.33)	246.7 (65.14)	134.6 (0.31)	317
51d	8.29	8.69	e (1)	136 (52.77) [b]	277.0 (100.44)	138.2 (0.36)	326
51e	12.40	13.27	b (1)	125 (74.92)	277.9 (86.31)	139.3 (0.23)	330
52a			an		215.5 (59.82)	129.0 (0.28)	315
52b	3.67	3.70	w (1)	84 (114.49)	143.8 (24.57)	128.9 (0.26)	316
53			an		253.6 (99.90)	130.0 (0.33)	301
54			an		260.7 (74.31)	132.8 (0.15)	296

[a] = solvents are abbreviated as follows: w = water, b = 2-butanol, as = anisole, an = anhydrous, e = ethanol, and their mole fraction is in parentheses; T_{ds} = desolvation T (°C), T_m = melting T (°C), T_d = decomposition T (°C) and their enthalpies ΔH (J g^{-1}); T_g = glass transition T taken from the 2nd heating scan and its ΔC_p (J g^{-1} °C^{-1}); [b] = recrystallization immediately after desolvation.

For the deoxycholic acid conjugate **50** four different forms were observed. Of these four forms three distinct crystalline modifications were identified. **50a** was a monohydrate whose SS-NMR analysis indicated that two non-equivalent molecules possibly existed in the asymmetric unit. This was suggested based on the doublet resonance patterns observed in the spectrum of **50a**. **50b**, for one, crystallized as a 2-butanol solvate along with traces of the hydrate **50a**. Only single resonances were visible in the SS-NMR spectrum of **50b**, including those

assigned for the solvent. Interestingly, the form obtained from anisole was dependent on the concentration used in the crystallization experiments. When a 2 % w/v anisole solution of **50** was used, a semi-crystalline anisole solvate **50c** was obtained, whereas the use of a 0.25 % w/v concentration resulted in the hydrate **50a**. As can be seen in Figure 16, the carbonyl carbon of the semi-crystalline anisole solvate **50c** possesses a triplet resonance pattern in its SS-NMR spectrum. The TG analysis supported the assumption that three distinct moieties may exist in the asymmetric unit, although the weight loss was lower than equal to $^1/_3$ moles of anisole (Table 4), which may be caused by amorphous content in the sample. The ^{13}C SS-NMR spectra of the different crystal modifications of compound **50** are shown in Figure 16.

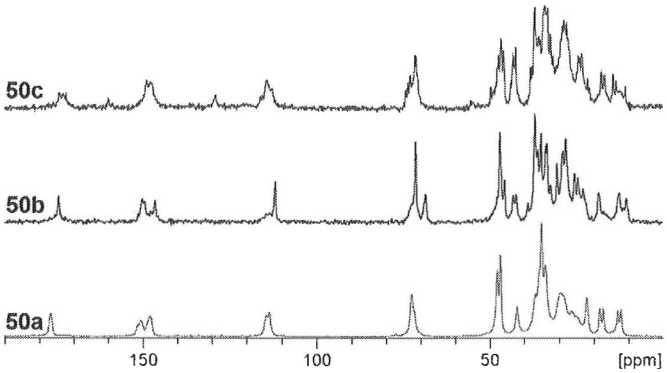

Figure 16. ^{13}C SS-NMR spectra of the different crystal modifications of the deoxycholyl-*N*-(4-aminopyridyl)amide **50**.

The cholic acid conjugate **51** is able to crystallize in at least five different crystalline forms; including an anhydrous form **51a**, a dihydrate **51b**, a monohydrate **51c**, an ethanol solvate **51d**, and a 2-butanol solvate **51e**. Since the SS-NMR spectrum of the aged hydrate **51c** resembled that of the anhydrous form **51a**, the XRD pattern was re-measured for the aged sample in order to rule out the possibility of a solid state phase transition from a kinetically stable to a thermodynamically more stable form. An XRD pattern of the hydrate equal to that of the original was produced, suggesting that care must be taken when interpreting the SS-NMR spectra and that the findings should preferably be confirmed by other methods. The ^{13}C SS-NMR spectra of the crystal modifications of compound **51** are shown in Figure 17.

An anhydrous form (**52a**) of the chenodeoxycholic acid conjugate **52** was obtained from five different solvent mixtures (Table 3). In addition, a hydrate **52b** was obtained from a saturated AcCN solution. Unfortunately, this form was isolated only once. The TG analysis showed that **52b** has an exceptionally low melting point compared to the other conjugates (Table 4), which indicates a highly metastable nature for this form. The ^{13}C SS-NMR spectra of forms **52a** and **52b** are shown in Figure 18.

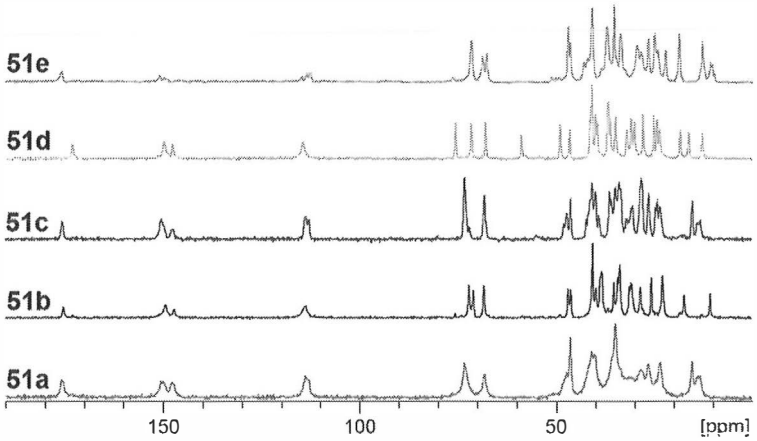

Figure 17. ^{13}C SS-NMR spectra of the different crystal modifications of the cholyl-*N*-(4-aminopyridyl)amide **51**.

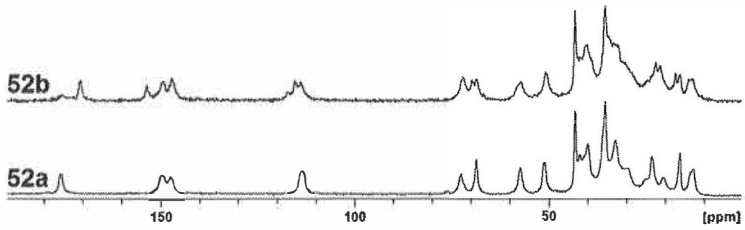

Figure 18. ^{13}C SS-NMR spectra of the different crystal modifications of the chenodeoxycholyl-*N*-(4-aminopyridyl)amide **52** (**52a** = anhydrous form and **52b** = hydrate form).

The ursodeoxycholic acid conjugate **53** and the hyodeoxycholic acid conjugate **54** crystallized as anhydrous forms regardless of the solvent systems used. Moreover, high quality crystals of conjugate **53** suitable for single crystal XRD experiment were obtained from ethanol/acetone and ethanol/water solutions. Crystal packing of compound **53** is shown in Figure 19. Hydrogen bonds N24-H···O3 and O7-H···O24 organize the molecules into right-handed helical chains.

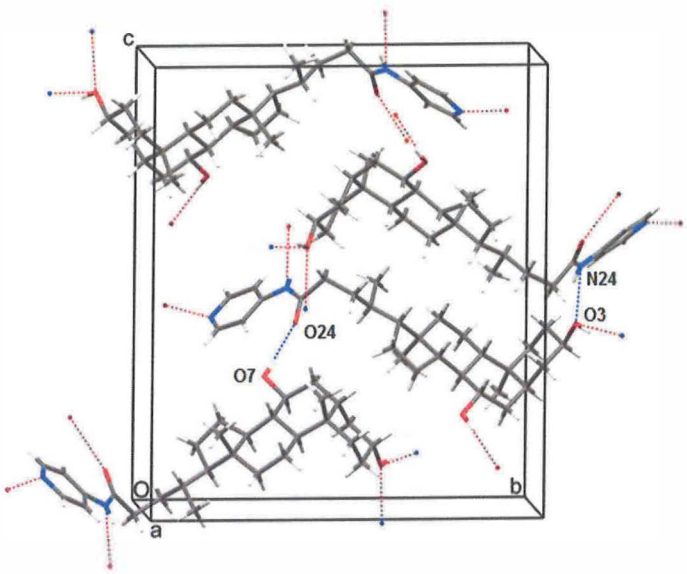

Figure 19. Crystal packing of ursodeoxycholyl-*N*-(4-aminopyridyl)amide **53**.

3.4 Computational studies of isocytosine and pyridine derivatives

Intrigued by the versatile solid state modifications of the selected pyridine derivatives observed experimentally, and described above in Chapter 3.3, we decided to study the ability of the theoretical methods to reproduce the solid state NMR parameters starting from the single crystal XRD data. Quantum chemical SS-NMR chemical shielding calculations were performed for two pyridine-derived compounds as well as for isocytosine. The geometry optimizations and calculations of the SS-NMR parameters were performed using the DFT-based CASTEP (Cambridge Serial Total Energy Package) and NMR-CASTEP programs, respectively.[223] The positions of the hydrogen atoms were optimized with the Broyden-Fletcher-Goldfarb-Shanno (BFGS) method[224-227] applying "ultrasoft" pseudopotentials[228], keeping the heavy atoms and the lattice volume fixed. The gauge-including projector-augmented wave (GIPAW)[229] procedure was used for the prediction of the magnetic resonance parameters. The electric field gradients and chemical shielding tensors were calculated for ^{13}C and ^{15}N nuclei for the geometry optimized structures and for the original X-ray structures.

3.4.1 CASTEP calculations for isocytosine[IV]

Based on its X-ray structure[230], neutral isocytosine crystallizes in a 1:1 ratio of two tautomers (Figure 20). The assignment of solid state NMR resonances of isocytosine was completed using NQS (non-quaternary suppression) and FSLG-HETCOR (frequency-switched Lee–Goldburg heteronuclear correlation) experiments. The ^{13}C and ^{15}N NMR chemical shifts were calibrated using carbonyl (at 176.03 ppm) and amine (at 32.1 ppm) resonances of glycine, respectively.

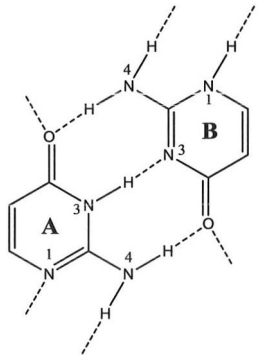

Figure 20. The two tautomers of isocytosine. Hydrogen bonds are shown by dashed lines.

CASTEP calculations were conducted using a normal workplace PC, and because of its limited memory capacity, positions of hydrogen atoms were optimized step by step. Optimization was initiated with a plane wave cut-off energy of 270 eV and the resulting structure was used for the next optimization step with a higher cut-off energy. The final optimized structure as well as the NMR parameters were calculated with a cut-off energy of 440 eV. The absolute shielding values obtained by NMR-CASTEP calculations were compared to the experimental NMR chemical shifts using linear correlation.

Compared to calculations performed for isolated isocytosine molecules or for isocytosine clusters, the GIPAW method was discovered to be able to reproduce the experimental data the most accurately. These calculations, which were based on the single crystal X-ray structure, however, were not accurate in predicting the chemical shifts of the nitrogens, which is why the positions of the hydrogen atoms were optimized. After the optimization, the N-H bond lengths were observed to have increased by a value of approximately 0.1 Å, which considerably improved the accuracy of the predicted chemical shifts of the nitrogens (Table 5).

Table 5. The experimental and calculated NMR chemical shift data: A = 3-NH, B = 1-NH (for numbering see Figure 20), c- = calculated without hydrogen position optimization, c+ = calculated with hydrogen position optimization, Δ = chemical shift difference compared to the experimental value.

Atom	A	ΔA/c-	ΔA/c+	B	ΔB/c-	ΔB/c+
C2	156.9	-0.5	0.0	156.9	-3.7	-2.4
C4	166.9	-1.4	+0.2	173.0	-0.1	-1.0
C5	101.4	+1.7	+0.7	105.4	-1.1	+1.0
C6	156.9	-0.4	+2.1	137.6	-0.4	+2.7
N1	195.5	+2.7	+2.1	122.1	-15.6	-0.1
N3	151.6	-10.6	-3.5	201.5	+4.5	-0.3
N4	82.2	-22.4	+0.1	78.8	-24.8	-1.0

3.4.2 CASTEP calculations for 2-alkanamido-6-[1*H*]-pyridones[V]

2-propanamido-6-pyridone **61** crystallized with two unequivalent molecules in the asymmetric unit. This was also evidenced by SS-NMR spectroscopy, which displayed double resonances with equal intensities in the spectrum (Figure 21, Table 6). 2-*Iso*-butanamido-6-pyridone **62** crystallized with only one molecule in the asymmetric unit (Figure 21, Table 7).

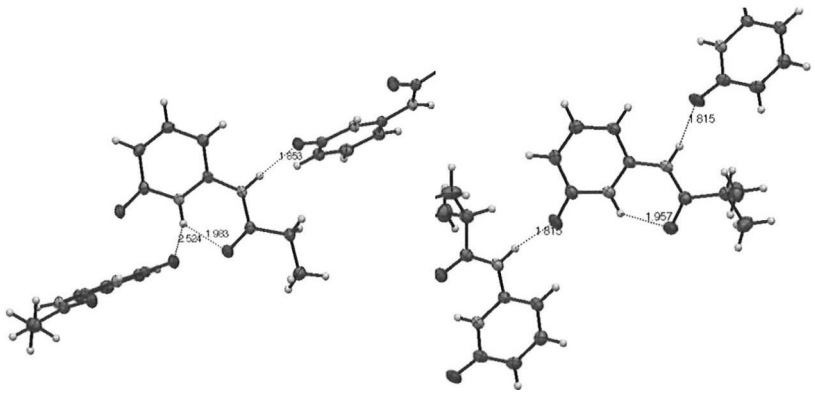

Figure 21. Crystal packing of 2-propanamido-6-pyridone **61** (left) and 2-*iso*-butanamido-6-pyridone **62** (right). Hydrogen bonds are shown by dashed lines.

As in the case of isocytosine, the GIPAW method was used to calculate the NMR chemical shielding parameters for the X-ray structures (**61a**, **62a**) as well as for the structures with optimized hydrogen positions (**61b**, **62b**). The absolute shielding values obtained by NMR-CASTEP calculations were changed to chemical shifts using the values calculated for glycine. All CASTEP calculations were performed using the supercomputing environment provided

by CSC – IT Center for Science Ltd., and the same cut-off energies were used for the geometry optimizations and for the NMR calculations. The optimization was performed at a cut-off energy of 440 eV for **61b** and **62b**, but since this cut-off energy seemed to underestimate the absolute shielding of the pyridine nitrogen in **62b**, a cut-off energy value of 550 eV was used for **62c**. This resulted in a fairly accurate estimation of the shielding for this nitrogen. Optimization of the structures, however, resulted in an underestimation of 10 ppm of the absolute shielding of the amide nitrogen donor of the hydrogen bond, and therefore the N-H bond length was fixed between the non-optimized and optimized structures (Table 8, **61c**, **62d**). This was observed to result in a high correspondence between the theoretical and experimental values. As can be seen in Table 8, the principal tensor component δ_{22} was the most sensitive for hydrogen bonding.

Table 6. Comparison of the SS-NMR chemical shift data. **61**(exp.) = experimental chemical shifts, **61a** = calculated for the crystal structure, **61b** = calculated after optimization of the location of the hydrogen atoms, and **61c** = calculated for **61b** with a fixed N1H1···O hydrogen bond length. The ^{13}C and ^{15}N NMR chemical shifts were calibrated using carbonyl (at 176.03 ppm) and amine (at -347.4 ppm) resonances of glycine, respectively.

Atom	**61**(exp.)	**61a**	**61b**	**61c**
C2	145.8	143.5	145.7	145.0
C2'	145.8	143.7	146.0	145.3
C3	93.6	87.5	95.6	94.9
C3'	93.6	87.7	95.6	94.9
C4	145.1	142.9	146.5	146.3
C4'	145.1	143.1	146.6	146.4
C5	111.2	108.3	113.2	114.0
C5'	112.1	110.2	114.8	115.5
C6	162.5	161.3	160.1	160.1
C6'	162.5	161.8	160.3	160.5
C9	174.9	174.7	176.2	175.9
C9'	175.2	175.4	176.8	176.6
CH_2	27.4	10.2	25.7	25.5
CH_2'	28.0	11.1	26.9	26.6
CH_3	7.5	-19.7	3.9	3.7
CH_3'	7.9	-19.2	4.7	4.6
N1	-222.7	-237.3	-220.6	-223.0
N1'	-221.2	-236.0	-223.2	-220.4
N8	-250.4	-255.4	-240.9	-251.4
N8'	-248.2	-253.5	-238.7	-249.7

Table 7. Comparison of the SS-NMR chemical shift data. **62**(exp.) = experimental chemical shifts, **62a** = calculated for the crystal structure, **62b** = calculated after optimization of the location of the hydrogen atoms at a cut-off energy of 440 eV, **62c** = calculated after optimization of the location of the hydrogen atoms at a cut-off energy of 550 eV, and **62d** = calculated for **62c** with a fixed N1H1···O hydrogen bond length. The ^{13}C and ^{15}N NMR chemical shifts were calibrated using carbonyl (at 176.03 ppm) and amine (at -347.4 ppm) resonances of glycine, respectively.

Atom	**62**(exp.)	**62a**	**62b**	**62c**	**62d**
C2	145.3	144.4	146.8	146.8	146.1
C3	94.9	90.0	97.3	97.2	96.6
C4	142.4	139.7	143.2	143.2	142.9
C5	111.0	107.4	112.6	112.5	113.1
C6	160.3	158.2	156.7	156.6	157.0
C9	179.1	180.7	180.4	180.3	180.0
methine CH	35.4	24.7	35.3	35.1	34.7
CH_3'	21.9	-3.9	20.8	20.7	20.7
CH_3	18.6	-8.7	16.5	16.4	16.2
N1	-223.1	-239.5	-212.9	-222.5	-222.8
N8	-250.2	-257.2	-241.1	-240.7	-252.1

Table 8. The effect of the hydrogen bond length (Å) on the principal shielding tensor components (ppm).

	61a	**61b**	**61c**	**62a**	**62c**	**62d**
N1H1···O	1.85/1.85	1.70/1.70	1.80/1.80	1.82	1.65	1.76
δ_{11}	175.1/175.6	164.3/164.4	174.7/174.2	179.0	167.6	179.0
δ_{22}	151.8/152.7	124.8/126.1	142.9/143.7	153.4	124.4	143.0
δ_{33}	-29.3/-25.2	-36.0/-30.8	-31.8/-26.8	-23.9	-32.9	-28.8

4 SUMMARY

Lithocholyl-*N*-(2-aminoethyl)amide (**36**) was shown to have a tendency to incorporate solvent molecules into its structure. The crystallization studies yielded solvates with *p*-xylene (**36b**), *iso*-propanol (**36c**), diethyl ether (**36d**), and chlorobenzene (**36e**). Amides of isomeric aminopyridines and lithocholic acid, on the other hand, crystallized solely as anhydrous forms or hydrates. Within the series of the aminopyridyl amides two single crystal X-ray structures (**37a**, **39a**) and one structure based on powder X-ray data (**39b**) were solved. Furthermore, in order to investigate the thermal stability of the crystallized forms, SS-NMR spectra were re-measured after a period of time revealing two opposite phenomena: the metastable dihydrate **38a** changed to an anhydrous form **38b**, whereas the anhydrous form **39a** changed to a hemi-trihydrate **39c**.

Systematic crystallization screening was conducted for five bile acid-4-aminopyridine conjugates resulting in twelve different crystal modifications. These modifications were extensively studied by means of solid state NMR, Raman, and IR spectroscopies, powder and single crystal X-ray diffraction methods, thermogravimetry, and differential scanning calorimetry. The cholic acid conjugate **51** was proven to have the highest tendency to crystallize as different modifications, resulting in an anhydrous form **51a**, a dihydrate **51b**, a monohydrate **51c**, an ethanol solvate **51d**, and a 2-butanol solvate **51e**. For the deoxycholyl derivative **50**, three distinct modifications were identified. The chenodeoxycholyl derivative **52** crystallized as an anhydrous form together with a hydrate, whereas for the urso- and hyodeoxycholyl derivatives (**53** and **54**, respectively) solely anhydrous forms were detected.

Infinite crystal calculations were conducted for a series of three nitrogen heterocycles in order to compare the single crystal structures to SS-NMR data. Optimization of hydrogen positions of the X-ray structure turned out to be essential especially in the case of hydrogen bonds. Furthermore, the position of the amide proton needed manual adjustment in the case of 2-acylamino-6-[1*H*]-pyridones (**61**, **62**) in order to obtain accurate results.

The current work provides important information about the solid state behavior of amides of bile acids with potential pharmaceutical activity. Because different crystal modifications of one molecule may possess distinct physico-chemical properties influencing, e.g., its stability over time or its bioavailability, it is essential to identify and characterize these forms. Moreover, the ability of the NMR-CASTEP program to reliably predict SS-NMR chemical shifts for nitrogen heterocycles was demonstrated. This can prove useful in interpreting complicated experimental problems where precise locations of hydrogen atoms of the molecule are required.

REFERENCES

1. http://ntp.niehs.nih.gov/ntp/htdocs/Chem_Background/ExSumPdf/aminopyridines.pdf (25.5.2012)

2. http://www.cdc.gov/niosh/docs/81-123/pdfs/0026-rev.pdf (25.5.2012)

3. M.W. Whitehouse, *Br. J. Clin. Pharmacol.*, **1986**, *22*(Suppl. 2), 111S-116S.

4. S. Peng, N.M. Okeley, A.-L. Tsai, G. Wu, R.J. Kulmacz and W.A. van der Donk, *J. Am. Chem. Soc.*, **2002**, *124*, 10785-10796.

5. J.L. Wallace, *Physiol. Rev.*, **2008**, *88*, 1547-1565.

6. R.J. Vane, Y.S. Bakhle and R.M. Botting, *Annu. Rev. Pharmacol. Toxicol.*, **1998**, *38*, 97-120.

7. G.P. O'Neill and A.W. Ford-Hutchinson, *FEBC lett.*, **1993**, *330*, 156-160.

8. Y. Tasaki, J. Yamamoto, T. Omura, T. Noda, N. Kamiyama, K. Yoshida, M. Satomi, T. Sakaguchi, M. Asari, T. Ohkubo, K. Shimizu and K. Matsubara, *Eur. J. Pharmacol.*, **2012**, *676*, 57-63.

9. S. Timmons, M.F. Coakley, A.M. Moloney and C. O'Neill, *Neurosci. Lett.*, **2009**, *467*, 30-35.

10. J.G. Lombardino, *Bull. Hist. Chem.*, **2000**, *25*, 10-15.

11. http://labeling.pfizer.com/ShowLabeling.aspx?id=569 (25.5.2012)

12. http://labeling.pfizer.com/ShowLabeling.aspx?id=750 (25.5.2012)

13. J.E. Polli, S. Bigora, D.A. Piscitelli, A.B. Straughn and D. Young, *Biopharm. Drug Dispos.*, **1996**, *17*, 635–641.

14. M. Tvrdonova, L. Dedik, C. Mircioiu, D. Miklovicova and M. Durisova, *Bas. Clin. Pharmacol. Toxicol.*, **2008**, *104*, 35-42.

15. F. Richy, C. Scarpignato, A. Lanas and J.-Y. Reginster, *Pharmacol. Res.*, **2009**, *60*, 254-263.

16. E.A. Meade, W.L. Smith and D.L. DeWitt, *J. Biol. Chem.*, **1993**, *268*, 6610-6614.

17. O.M. Laudanno, J.A. Cesolari, J. Esnarriaga, P. San Miguel and O.A. Bedini, *Dig. Dis. Sci.*, **2000**, *45*, 1359-1365.

18. C.J. Hawkey, *Lancet*, **1999**, *353*, 307-314.

19. W.N. William, J.V. Heymach, E.S. Kim and S.M. Lippman, *Nat. Rev. Drug Disc.*, **2009**, *8*, 213-225.

20. D.G. Menter, R.L. Schilsky and R.N. DuBois, *Clin. Cancer Res.*, **2010**, *16*, 1384-1390.

21. S.J. Shiff, M.I. Koutsos, L. Qiao and B. Rigas, *Exp. Cell Res.*, **1996**, *222*, 179–188.

22. R. Ettarh, A. Cullen and A. Calamai, *Pharmaceuticals*, **2010**, *3*, 2007-2021.

23. S.I. Mohammed, P.F. Bennett, B.A. Craig, N.W. Glickman, A.J. Mutsaers, P.W. Snyder, W.R. Widmer, A.E. DeGortari, P.L. Bonney and D.W. Knapp, *Cancer Res.*, **2002**, *62*, 356-358.

24. J.C. Bulman-Fleming, T.R. Turner and M.P. Rosenberg, *J. Feline Med. Surg.*, **2010**, *12*, 262-268.

25. A. Mas, L. Blackwood, P. Cripps, S. Murphy, J. De Vos, N. Dervisis, M. Martano and G.A. Polton, *J. Small Anim. Pract.*, **2011**, *52*, 359–364.

26. K. Ravishankar, H. Tayade and R. Mandlik, *J. Assoc. Physicians India,* **2011**, *59*, 494-497.

27. L. Patoia, L. Santucci, P. Furno, M.S. Dionisi, S. Dell'Orso, M. Romagnoli, A. Sattarinia and M.G. Marini, *Br. J. Rheumatol.*, **1996**, *35*(Suppl. 1), 61-67.

28. T.J. Carty, A. Marfat, P.F. Moore, F.C. Falkner, T.M. Twomey and A. Weissman, *Agents Actions*, **1993**, *39*, 157-165.

29. J. Jayaselli, J.M.S. Cheemala, G. Rani D. P. and S. Pal, *J. Braz. Chem. Soc.*, **2008**, *19*, 509-515.

30. P.J. Riedemann, S. Bersinic, L.J. Cuddy, G.W. Torrance and P.X. Tugwell, *J. Rheumatol.*, **1993**, *20*, 2095-2103.

31. D.I. Nesseem, S.F. Eid and S.S. El-Houseny, *Life Sciences*, **2011**, *89*, 430-438.

32. R.I.M. Galvão, J.P.L. Diógenes, G.C.L. Maia, E.A.S. Filho, S.M.M. Vasconcelos, D.B. de Menezes, G.M.A. Cunha and G.S.B. Viana, *Neurochem. Res.*, **2005**, *30*, 39-46.

33. M. Naziroğlu, A.C. Uğuz, A. Gokçimen, M. Bülbül, D.U. Karatopuk, Y. Türker and C. Çerçi, *Neurochem. Res.*, **2008**, *33*, 1832-1837.

34. E.-M. Homdrum, R. Likar and G. Nell, *Eur. Surg.*, **2006**, *38*, 342-352.

35. E. Cevik, O. Cinar, N. Salman, A. Bayir, I. Arziman, S. Ardic and S.T. Youngquist, *Am. J. Emerg. Med.*, **2012**, In Press.

36. P. Byrav D.S., B. Medhi, A. Prakash, S. Patyar and S. Wadhwa, *Ind. J. Phys. Med. Rehab.*, **2009**, *20*, 27-31.

37. S.E. Nørholt, S. Sindet-Pedersen, U. Larsen, U. Bang, J. Ingerslev, O. Nielsen, H.J. Hansen and A.K. Ersbøll, *Pain*, **1996**, *67*, 335-343.

38. D.E. Rosenow, M. Albrechtsen and D. Stolke, *Anesth. Analg.*, **1998**, *86*, 1045-1050.

39. R.S. Jadon, S. Nayak, S. Amlan, V.D. Vaidya, P. Khemariya, S. Sumbhate and S. Nayak, *Int. J. Drug Del.*, **2009**, *1*, 27-31.

40. G. Cavallini, G. Biagiotti, A.P. Ferraretti, L. Gianaroli and G. Vitali, *Brit. J. Urol. Int.*, **2003**, *91*, 513-518.

41. G. Cavallini, A.P. Ferraretti, L. Gianaroli, G. Biagiotti and G. Vitali, *J. Androl.*, **2004**, *25*, 761-770.

42. R. Ficarra, A. Villari, N. Micali, S. Tommasini, M.L. Calabrò, M.R. Di Bella, S. Melardi, M.F. Agresta, S. Coppolino and R. Stancanelli, *J. Pharm. Biomed. Anal.*, **1999**, *20*, 283-288.

43. P.B. Dews and J.D.J. Graham, *Brit. J. Pharmacol.*, **1946**, *1*, 278-286.

44. M.E. Parsons and C.R. Ganellin, *Brit. J. Pharmacol.*, **2006**, *147*, S127-S135.

45. M. Shahid, T. Tripathi, F. Sobia, S. Moin, M. Siddiqui and R. Ali Khan, *Open Immunol. J.*, **2009**, *2*, 9-41.

46. F.E.R. Simons and K.J. Simons, *J. Allergy Clin. Immunol.*, **2011**, *128*, 1139-1150.

47. M.H. Levin, R.A. Weinstein, C. Nathan, R.K. Selander, H. Ochman and S.A. Kabins, *J. Clin. Microbiol.*, **1984**, *20*, 758-762.

48. P.J. Fudala and R.E. Johnson, *Drug Alcohol Depend.*, **2006**, *83S*, S40-S47.

49. I.A. Wasfi, A.A. Abdel Hadi, M. Elghazali, N.S. Boni, N.A. Alkatheeri, I.M. Barezaig, A.M. Al Muharami and A.M. Hamid, *J. Vet. Pharmacol. Therap.*, **2000**, *23*, 145-152.

50. L. Dirikolu, A.F. Lehner, J.D. Harkins, W.E. Woods, Karpiesiuk, R.S. Gates, M. Fisher and T. Tobin, *J. Vet. Pharmacol. Therap.*, **2009**, *32*, 66-78.

51. F.M. Villemain, J.-F. Bach and L.M. Chatenoud, *J. Immunol.*, **1990**, *144*, 1449-1454.

52. M. Ruat, M. Körner, M. Garbarg, C. Gros, J.C. Schwartz, W. Tertiuk and C.R. Ganellin, *Proc. Natl. Acad. Sci. USA*, **1988**, *85*, 2743-2747.

53. A. Samadi, J. Marco-Contelles, E. Soriano, M. Álvarez-Pérez, M. Chioua, A. Romero, L. González-Lafuente, L. Gandía, J.M. Roda, M.G. López, M. Villarroya, A.G. García and C. de los Ríos, *Bioorg. Med. Chem.*, **2010**, *18*, 5861-5872.

54. H. Ji, S.L. Deiker, H. Li, P. Martásek, L.J. Roman, T.L. Poulos and R.B. Silverman, *J. Med. Chem.*, **2010**, *53*, 7804-7824.

55. M. Racchi, M. Mazzucchelli, E. Porrello, C. Lanni and S. Govoni, *Pharmacol. Res.*, **2004**, *50*, 441-451.

56. C. Stevens, L. Smith and N.B. La Thangue, *Nat. Cell Biol.*, **2003**, *5*, 401-409.

57. S. Hilton, S. Naud, J.J. Caldwell, K. Boxall, S. Burns, V.E. Anderson, L. Antoni, C.E. Allen, L.H. Pearl, A.W. Oliver, G.W. Aherne, M.D. Garrett and I. Collins, *Bioorg. Med. Chem.*, **2010**, *18*, 707-718.

58. F.M. Matschinsky, *Nat. Rev. Drug Disc.*, **2009**, *8*, 399-416.

59. M.J. Waring, I.J. Brogan, M. Coghlan, C. Johnstone, H.B. Jones, B. Leighton, D. McKerrecher, K.G. Pike and G.R. Robb, *Med. Chem. Commun.*, **2011**, *2*, 771-774.

60. J.A. Pfefferkorn, A. Guzman-Perez, J. Litchfield, R. Aiello, J.L. Treadway, J. Pettersen, M.L. Minich, K.J. Filipski, C.S. Jones, M. Tu, G. Aspnes, H. Risley, J. Bian, B.D. Stevens, P. Bourassa, T. D'Aquila, L. Baker, N. Barucci, A.S. Robertson, F. Bourbonais, D.R. Derksen, M. MacDougall, O. Cabrera, J. Chen, A.L. Lapworth, J.A. Landro, W.J. Zavadoski, K. Atkinson, N. Haddish-Berhane, B. Tan, L. Yao, R.E. Kosa, M.V. Varma, B. Feng, D.B. Duignan, A. El-Kattan, S. Murdande, S. Liu, M. Ammirati, J. Knafels, P. DaSilva-Jardine, L. Sweet, S. Liras and T.P. Rolph, *J. Med. Chem.*, **2012**, *55*, 1318-1333.

61. D.L. Nelson and M.M. Cox, *Lehninger Principles of Biochemistry*, World Publishers, The United States of America, **2000**, p.449.

62. N. Tuteja, M. Chandra, R. Tuteja and M.K. Misra, *J. Biomed. Biotech.*, **2004**, *4*, 227-237.

63. E.D. Garcin, A.S. Arvai, R.J. Rosenfeld, M.D. Kroeger, B.R. Crane, G. Andersson, G. Andrews, P.J. Hamley, P.R. Mallinder, D.J. Nicholls, S.A. St-Gallay, A.C. Tinker, N.P. Gensmantel, A. Mete, D.R. Cheshire, S. Connolly, D.J. Stuehr, A. Åberg, A.V. Wallace, J.A. Tainer and E.D. Getzoff, *Nat. Chem. Biol.*, **2008**, *4*, 700-707.

64. G.J. Southan, A.L. Salzman and C. Szabó, *Pharmacol. Commun.*, **1996**, *7*, 275-286.

65. W.S. Faraci, A.A. Nagel, K.A. Verdries, L.A. Vincent, H. Xu, L.E. Nichols, J.M. Labasi, E.D. Salter and E.R. Pettipher, *Br. J. Pharmacol.*, **1996**, *119*, 1101-1108.

66. R.A. Finch, M.-C. Liu, A.H. Cory, J.G. Cory and A.C. Sartorelli, *Advan. Enzyme Regul.*, **1999**, *39*, 3-12.

67. R.A. Finch, M.-C. Liu, S.P. Grill, W.C. Rose, R. Loomis, K.M. Vasquez, Y.-C. Cheng and A.C. Sartorelli, *Biochem. Pharmacol.*, **2000**, *59*, 983-991.

68. Y. Yu, J. Wong, D.B. Lovejoy, D.S. Kalinowski and D.R. Richardson, *Clin. Cancer Res.*, **2006**, *12*, 6876-6883.

69. S. Attia, J. Kolesar, M.R. Mahoney, H.C. Pitot, D. Laheru, J. Heun, W. Huang, J. Eickhoff, C. Erlichman and K.D. Holen, *Invest. New Drugs*, **2008**, *26*, 369-379.

70. J.J. Knox, S.J. Hotte, C. Kollmannsberger, E. Winquist, B. Fisher and E.A. Eisenhauer, *Invest. New Drugs*, **2007**, *25*, 471-477.

71. I. Gojo, M.L. Tidwell, J. Greer, N. Takebe, K. Seiter, M.F. Pochron, B. Johnson, M. Sznol and J.E. Karp, *Leukemia Res.*, **2007**, *31*, 1165-1173.

72. C.M. Nutting, C.M.L. van Herpen, A.B. Miah, S.A. Bhide, J.-P. Machiels, J. Buter, C. Kelly, D. de Raucourt and K.J. Harrington, *Ann. Oncol.*, **2009**, *20*, 1275-1279.

73. J. Chao, T.W. Synold, R.J. Morgan Jr., C. Kunos, J. Longmate, H.-J. Lenz, D. Lim, S. Shibata, V. Chung, R.G. Stoller, C.P. Belani, D.R. Gandara, M. McNamara, B.J. Gitlitz, D.H. Lau, S.S. Ramalingam, A. Davies, I. Espinoza-Delgado, E.M. Newman and Y. Yen, *Cancer Chemother. Pharmacol.*, **2012**, *69*, 835-843.

74. A.J. Ocean, P. Christos, J.A. Sparano, D. Matulich, A. Kaubish, A. Siegel, M. Sung, M.M. Ward, N. Hamel, I. Espinoza-Delgado, Y. Yen and M.E. Lane, *Cancer Chemother. Pharmacol.*, **2011**, *68*, 379-388.

75. B. Ma, B.C. Goh, E.H. Tan, K.C. Lam, R. Soo, S.S. Leong, L.Z. Wang, F. Mo, A.T.C. Chan, B. Zee and T. Mok, *Invest. New Drugs*, **2008**, *26*, 169-173.

76. A.M. Traynor, J.-W. Lee, G.K. Bayer, J.M. Tate, S.P. Thomas, M. Mazurczak, D.L. Graham, J.M. Kolesar and J.H. Schiller, *Invest. New Drugs*, **2010**, *28*, 91-97.

77. J.E. Karp, F.J. Giles, I. Gojo, L. Morris, J. Greer, B. Johnson, M. Thein, M. Sznol and J. Low, *Leukemia Res.*, **2008**, *32*, 71-77.

78. W.R. Schelman, S. Morgan-Meadows, R. Marnocha, F. Lee, J. Eickhoff, W. Huang, M. Pomplun, Z. Jiang, D. Alberti, J.M. Kolesar, P. Ivy, G. Wilding and A.M. Traynor, *Cancer Chemother. Pharmacol.*, **2009**, *63*, 1147-1156.

79. K.W.L. Yee, J. Cortes, A. Ferrajoli, G. Garcia-Manero, S. Verstovsek, W. Wierda, D. Thomas, S. Faderl, I. King, S.M. O'Brien, S. Jeha, M. Andreeff, A. Cahill, M. Sznol and F.J. Giles, *Leukemia Res.*, **2006**, *30*, 813-822.

80. O.M. Odenike, R.A. Larson, D. Gajria, M.E. Dolan, S.M. Delaney, T.G. Karrison, M.J. Ratain and W. Stock, *Invest. New Drugs*, **2008**, *26*, 233-239.

81. C.A. Kunos, S. Waggoner, V. von Gruenigen, E. Eldermire, J. Pink, A. Dowlati and T.J. Kinsella, *Clin. Cancer Res.*, **2010**, *16*, 1298-1306.

82. http://clinicaltrials.gov/ct2/show/study/NCT00941070?term=NCT00941070&rank=1 (25.5.2012)

83. G. Rappa, A. Lorico, M.-C. Liu, G.D. Kruh, A.H. Cory, J.G. Cory and A.C. Sartorelli, *Biochem. Pharmacol.*, **1997**, *54*, 649-655.

84. P. Heffeter, C. Pirker, C.R. Kowol, G. Herrman, R. Dornetshuber, W. Miklos, U. Jungwirth, G. Koellensperger, B.K. Keppler and W. Berger, *Biochem. Pharmacol.*, **2012**, *83*, 1623-1633.

85. T. Hallström and K. Riesbeck, *Trends Microbiol.*, **2010**, *18*, 258-265.

86. D.C. Turk, *J. Med. Microbiol.*, **1984**, *18*, 1-16.

87. G. Gerlach and J. Reidl, *J. Bacteriol.*, **2006**, *188*, 6719-6727.

88. E. Sauer, M. Merdanovic, A.P. Mortimer, G. Bringmann and J. Reidl, *Antimicrob. Agents Chemother.*, **2004**, *48*, 4532-4541.

89. http://epa.gov/oppsrrd1/REDs/aminopyridine_red.pdf (25.5.2012)

90. M.L. Avery, *Avian Repellents* in *Encyclopedia of Agrochemicals*, John Wiley & Sons, Hoboken, New Jersey, USA **2003**.

91. D.E. Williams and R.M. Corrigan, *The Handbook: Prevention and Control of Wildlife Damage*, **1994**, paper 69.

92. D.R. Jeffery and E.P. Pharr, *Core Evidence*, **2010**, *5*, 107-112.

93. M. Pugliatti, S. Sotgiu and G. Rosati, *Clin. Neurol. Neurosurg.*, **2002**, *104*, 182-191.

94. A. Compston and A. Coles, *Lancet*, **2008**, *372*, 1502-1517.

95. http://www.fda.gov/NewsEvents/Newsroom/PressAnnouncements/ucm198463.htm (25.5.2012)

96. S.I.V. Judge and C.T. Bever Jr., *Pharmacol. Ther.*, **2006**, *111*, 224-259.

97. A.D. Goodman, T.R. Brown, L.B. Krupp, R.T. Schapiro, S.R. Schwid, R. Cohen, L.N. Marinucci and A.R. Blight, *Lancet*, **2009**, *373*, 732-738.

98. A.D. Goodman, T.R. Brown, K.R. Edwards, L.B. Krupp, R.T. Schapiro, R. Cohen, L.N. Marinucci and A.R. Blight, *Ann. Neurol.*, **2010**, *68*, 494-502.

99. http://clinicaltrials.gov/ct2/show/NCT01399957?term=dalfampridine&rank=10 (25.5.2012)

100. A.R. Blight, *Ther. Adv. Neurol. Disord.*, **2011**, *4*, 99-109.

101. A.D. Goodman, J.A. Cohen, A. Cross, T. Vollmer, M. Rizzo, R. Cohen, L. Marinucci and A.R. Blight, *Mult. Scler.*, **2007**, *13*, 357-368.

102. J.M. Burton, C.M. Bell, S.E. Walker and P.W. O'Connor, *Neurology*, **2008**, *71*, 1833-1834.

103. E. Schwam, *J. Emerg. Med.*, **2011**, *41*, 51-54.

104. G. Leung, W. Sun, S. Brookes, D. Smith and R. Shi, *Exp. Neurol.*, **2011**, *227*, 232-235.

105. M.A.M. van der Bruggen, H.B.M. Huisman, H. Beckerman, F.W. Bertelsmann, C.H. Polman and G.J. Lankhorst, *J. Neurol.*, **2001**, *248*, 665-671.

106. R. Shi and A.R. Blight, *Neurosci.*, **1997**, *77*, 553-562.

107. J.M. McBride, D.T. Smith, S.R. Byrn, R.B. Borgens and R. Shi, *Neurosci.*, **2007**, *148*, 44-52.

108. H. Haghdoost-Yazdi, A. Faraji, N. Fraidouni, M. Movahedi, E. Hadibeygi and F. Vaezi, *Behav. Brain Res.*, **2011**, *223*, 70-74.

109. M. Keogh, S. Sedehizadeh and P. Maddison, *Cochrane Database of Systematic Reviews*, **2011**, *2*, 1-27.

110. W. Sun, D. Smith, Y. Fu, J.-X. Cheng, S. Bryn, R. Borgens and R. Shi, *J. Neurophysiol.*, **2010**, *103*, 469-478.

111. D.T. Smith, R. Shi, R.B. Borgens, J.M. McBride, K. Jackson and S.R. Byrn, *Eur. J. Med. Chem.*, **2005**, *40*, 908-917.

112. A. Andreani, A. Leoni, A. Locatelli, R. Morigi, M. Rambaldi, C. Pietra and G. Villetti, *Eur. J. Med. Chem.*, **2000**, *35*, 77-82.

113. H. Lundh, O. Nilsson and I. Rosén, *J. Neurol. Neurosurg. Psychiatry*, **1979**, *42*, 171-175.

114. M.N. Meriggioli and D.B. Sanders, *Lancet Neurol.*, **2009**, *8*, 475-490.

115. R. Hourez, L. Servais, D. Orduz, D. Gall, I. Millard, A. de Kerchove d'Exaerde, G. Cheron, H.T. Orr, M. Paldolfo and S.N. Schiffmann, *J. Neurosci.*, **2011**, *31*, 11795-11807.

116. H.Y. Zoghbi and H.T. Orr, *J. Biol. Chem.*, **2009**, *284*, 7425-7429.

117. L.A. Fieber, D.M. González, M.R. Wallace and D. Muir, *Neurobiol. Dis.*, **2003**, *13*, 136-146.

118. L.S. Chin, C.C. Park, K.M. Zitnay, M. Sinha, A.J. DiPatri Jr., P. Perillán and J.M. Simard, *J. Neurosci. Res.*, **1997**, *48*, 122-127.

119. W. Wang, JB. Xiao, M. Adachi, Z. Liu and J. Zhou, *Cell. Physiol. Biochem.*, **2011**, *28*, 199-208.

120. M.J. Monte, J.J.G. Marin, A. Antelo and J. Vazquez-Tato, *World J. Gastroenterol.*, **2009**, *15*, 804-816.

121. P.B. Hylemon, H. Zhou, W.M. Pandak, S. Ren, G. Gil and P. Dent, *J. Lipid Res.*, **2009**, *50*, 1509-1520.

122. H. Wang, J. Chen, K. Hollister, L.C. Sowers and B.M. Forman, *Mol. Cell*, **1999**, *3*, 543-553.

123. M. Makishima, A.Y. Okamoto, J.J. Repa, H. Tu, R.M. Learned, A. Luk, M.V. Hull, K.D. Lustig, D.J. Mangelsdorf and B. Shan, *Science*, **1999**, *284*, 1362-1365.

124. D.J. Parks, S.G. Blanchard, R.K. Bledsoe, G. Chandra, T.G. Consler, S.A. Kliewer, J.B. Stimmel, T.M. Willson, A.M. Zavacki, D.D. Moore and J.M. Lehmann, *Science*, **1999**, *284*, 1365-1368.

125. Y. Kawamata, R. Fujii, M. Hosoya, M. Harada, H. Yoshida, M. Miwa, S. Fukusumi, Y. Habata, T. Itoh, Y. Shintani, S. Hinuma, Y. Fujisawa and M. Fujino, *J. Biol. Chem.*, **2003**, *278*, 9435-9440.

126. S. Katsuma, A. Hirasawa and G. Tsujimoto, *Biochem. Biophys. Res. Commun.*, **2005**, *329*, 386-390.

127. K. Cheng, Y. Chen, P. Zimniak, J.-P. Raufman, Y. Xiao and H. Frucht, *Biochim. Biophys. Acta*, **2002**, *1588*, 48-55.

128. J.-P. Raufman, Y. Chen, K. Cheng, C. Compadre, L. Compadre and P. Zimniak, *Eur. J. Pharmacol.*, **2002**, *457*, 77-84.

129. S.H. Sheikh Abdul Kadir, M. Miragoli, S. Abu-Hayyeh, A.V. Moshkov, Q. Xie, V. Keitel, V.O. Nikolaev, C. Williamson and J. Gorelik, *PLoS ONE*, **2010**, *5*, e9689.

130. E.C. von Rosenvinge and J.-P. Raufman, *Cancers*, **2011**, *3*, 971-981.

131. M. Ogundare, S. Theofilopoulos, A. Lockhart, L.J. Hall, E. Arenas, J. Sjövall, A.G. Brenton, Y. Wang and W.J. Griffiths, *J. Biol. Chem.*, **2010**, *285*, 4666-4679.

132. A.F. Hofmann and K.J. Mysels, *J. Lipid Res.*, **1992**, *33*, 617-626.

133. A.F. Hofmann and L.R. Hagey, *Cell Mol. Life Sci.*, **2008**, *65*, 2461-2483.

134. E. Sievänen, *Molecules*, **2007**, *12*, 1859-1889.

135. G.J. Jenkins and L.J. Hardie (eds.), *Bile Acids: Toxicity and Bioactivity*, Royal Society of Chemistry, Cambridge, **2008**, pp. 176.

136. L. Yang, J.P. Fawcett, J. Østergaard, H. Zhang and I.G. Tucker, *Mol. Pharmaceutics*, **2012**, *9*, 29-36.

137. K.R. Jadhav, M.N. Gambhire, I.M. Shaikh, V.J. Kadam and S.S. Pisal, *Curr. Drug Ther.*, **2007**, *2*, 27-38.

138. C. Naveen, Y.K. Kumar, P.V. Rao and T.R. Rao, *Int. J. Pharm. Sci. Nanotech.*, **2011**, *4*, 1307-1319.

139. *J. Cell. Biochem.*, **1996**, *63*(Suppl. 26), 258-268.

140. http://www.aptalispharma.com/pdf/rap97.pdf (24.7.2012)

141. K.D. Lindor, M.E. Gershwin, R. Poupon, M. Kaplan, N.V. Bergasa and E.J. Heathcote, *Hepatology*, **2009**, *50*, 291-308.

142. W.H. Bachrach and A.F. Hofmann, *Dig. Dis. Sci.*, **1982**, *27*, 833-856.

143. N.G. Venneman, M.G.H. Besselink, Y.C.A. Keulemans, G.P. van Berge-Henegouwen, M.A. Boermeester, I.A.M.J. Broeders, P.M.N.Y.H. Go and K.J. van Erpecum, *Hepatology*, **2006**, *43*, 1276-1283.

144. M.C. Uy, M.C. Talingdan-Te, W.Z. Espinosa, M.L.O. Daez and J.P. Ong, *Obes. Surg.*, **2008**, *18*, 1532-1538.

145. M.M. Kaplan and M.E. Gershwin, *N. Engl. J. Med.*, **2005**, *353*, 1261-1273.

146. K. Dilger, S. Hohenester, U. Winkler-Budenhofer, B.A.J. Bastiaansen, F.G. Schaap, C. Rust and U. Beuers, *J. Hepatol.*, **2012**, *57*, 133-140.

147. H. Jackson, M. Solaymani-Dodaran, T.R. Card, G.P. Aithal, R. Logan and J. West, *Hepatology*, **2007**, *46*, 1131-1137.

148. M.G. Silveira and K.D. Lindor, *World J. Gastroenterol.*, **2008**, *14*, 3338-3349.

149. L. Okolicsanyi, M. Groppo, A. Floreani, A.M. Morselli-Labate, A.G. Rusticali, A. Battocchia, M. Colombo, G. Galatola, G. Gasbarrini, M. Podda, G. Ricci, F. Rosina and M. Zuin, *Dig. Liver Dis.*, **2003**, *35*, 325-331.

150. S.N. Cullen, C. Rust, K. Fleming, C. Edwards, U. Beuers and R.W. Chapman, *J. Hepatol.*, **2008**, *48*, 792-800.

151. E. Sinakos, H.-U. Marschall, K.V. Kowdley, A. Befeler, J. Keach and K. Lindor, *Hepatology*, **2010**, *52*, 197-203.

152. J.E. Eaton, M.G. Silveira, D.S. Pardi, E. Sinakos, K.V. Kowdley, V.A.C. Luketic, M.E. Harrison, T. McCashland, A.S. Befeler, D. Harnois, R. Jorgensen, J. Petz and K.D. Lindor, *Am. J. Gastroenterol.*, **2011**, *106*, 1638-1645.

153. A. Jemal, M.M. Center, C. DeSantis and E.M. Ward, *Cancer Epidemiol. Biomarkers Prev.*, **2010**, *19*, 1893-1907.

154. P. Pisani, D.M. Parkin, F. Bray and J. Ferlay, *Int. J. Cancer*, **1999**, *83*, 18-29.

155. M.M. Center, A. Jemal, R.A. Smith and E. Ward, *CA Cancer J. Clin.*, **2009**, *59*, 366-378.

156. R.A. Weinberg, *The Biology of Cancer*, Garland Science, New York, **2007**.

157. P. Gervaz, P. Bucher and P. Morel, *J. Surg. Oncol.*, **2004**, *88*, 261-266.

158. R. Solimando, F. Bazzoli and L. Ricciardiello, *Best Pract. Res. Clin. Gastroenterol.*, **2011**, *25*, 555-568.

159. P.A. Thompson, B.C. Wertheim, D.J. Roe, E.L. Ashbeck, E.T. Jacobs, P. Lance, M.E. Martinez and D.S. Alberts, *Cancer Prev. Res.*, **2009**, *2*, 1023-1030.

160. C.D. Keene, C.M.P. Rodrigues, T. Eich, C. Linehan-Stieers, A. Abt, B.T. Kren, C.J. Steer and W.C. Low, *Exp. Neurol.*, **2001**, *171*, 351-360.

161. R.M. Ramalho, P.M. Borralho, R.E. Castro, S. Solá, C.J. Steer and C.M.P. Rodrigues, *J. Neurochem.*, **2006**, *98*, 1610-1618.

162. R.M. Ramalho, R.J.S. Viana, W.C. Low, C.J. Steer and C.M.P. Rodrigues, *Trends Mol. Med.*, **2008**, *14*, 54-62.

163. J.D. Amaral, R.J.S. Viana, R.M. Ramalho, C.J. Steer and C.M.P. Rodrigues, *J. Lipid Res.*, **2009**, *50*, 1721-1734.

164. I.H. Park, M.K. Kim and S.U. Kim, *Biochem. Biophys. Res. Commun.*, **2008**, *377*, 1025-1030.

165. M.A. Brito, S. Lima, A. Fernandes, A.S. Falcão, R.F.M. Silva, D.A. Butterfield and D. Brites, *Neuro Toxicol.*, **2008**, *29*, 259-269.

166. L. Régal, M.S. Ebberink, N. Goemans, R.J.A. Wanders, L. De Meirleir, J. Jaeken, M. Schrooten, R. Van Coster and H.R. Waterham, *Ann. Neurol.*, **2010**, *68*, 259-263.

167. J. Haleblian and W. McCrone, *J. Pharm. Sci.*, **1969**, *58*, 911-929.

168. A. Gavezzotti, *J. Pharm. Sci.*, **2007**, *96*, 2232-2241.

169. D. Braga, F. Grepioni, L. Maini and M. Polito, *Struct. Bond*, **2009**, *132*, 25-50.

170. J. Thun, L. Seyfarth, J. Senker, R.E. Dinnebier and J. Breu, *Angew. Chem. Int. Ed.*, **2007**, *46*, 6729-6731.

171. J. Thun, L. Seyfarth, J. Senker, R.E. Dinnebier and J. Breu, *Cryst. Growth Des.*, **2009**, *9*, 2435-2441.

172. N. Blagden, R. Davey, G. Dent, M. Song, W.I.F. David, C.R. Pulham and K. Shankland, *Cryst. Growth Des.*, **2005**, *5*, 2218-2224.

173. J. Thun, M. Schoeffel and J. Breu, *Mol. Simulat.*, **2008**, *34*, 1359-1370.

174. R. Purohit and P. Venugopalan, *Resonance*, **2009**, *14*, 882-893.

175. F.H. Herbstein, *Cryst. Growth Des.*, **2004**, *4*, 1419-1429.

176. D. Braga, F. Grepioni and L. Maini, *Chem. Commun.*, **2010**, *46*, 6232-6242.

177. R. Hilfiker (ed.), *Polymorphism: in the Pharmaceutical Industry*, Wiley-VCH, Weinheim, **2006**.

178. A.Y. Lee, D. Erdemir and A.S. Myerson, *Ann. Rev. Chem. Biomol. Eng.*, **2011**, *2*, 259-280.

179. M. Suzuki and K. Kobayashi, *Cryst. Growth Des.*, **2011**, *11*, 1814-1820.

180. J. Bernstein, *Cryst. Growth Des.*, **2005**, *5*, 1661-1662.

181. C.B. Aakeröy and D.J. Salmon, *Cryst. Eng. Comm.*, **2005**, *7*, 439-448.

182. P. Vishweshwar, J.A. McMahon, M.L. Peterson, M.B. Hickey, T.R. Shattock and M.J. Zaworotko, *Chem. Commun.*, **2005**, *36*, 4601-4603.

183. A. Mukherjee and G.R. Desiraju, *Chem. Commun.*, **2011**, *47*, 4090-4092.

184. K. Fujii, H. Uekusa, N. Itoda, G. Hasegawa, E. Yonemochi, K. Terada, Z. Pan and K.D.M. Harris, *J. Phys. Chem. C*, **2010**, *114*, 580-586.

185. L.F. Kuyper and C.W. Carter Jr., *J. Cryst. Growth*, **1996**, *168*, 155-169.

186. J. Aaltonen, M. Allesø, S. Mirza, V. Koradia, K.C. Gordon and J. Rantanen, *Eur. J. Pharm. Biopharm.*, **2009**, *71*, 23-37.

187. J. Bernstein, R.J. Davey and J.-O. Henck, *Angew. Chem. Int. Ed.*, **1999**, *38*, 3440-3461.

188. S. Jiang, J.H. ter Horst and P.J. Jansens, *Cryst. Growth Des.*, **2008**, *8*, 37-43.

189. J. Čejka, A. Corma and S. Zones (eds.), *Zeolites and Catalysis, Synthesis, Reactions and Applications. Vol. 1.*, Wiley-VCH, Weinheim, **2010**.

190. D. Kashchiev and G.M. van Rosmalen, *Cryst. Res. Technol.*, **2003**, *38*, 555-574.

191. M. Kitamura, *Cryst. Growth Des.*, **2004**, *4*, 1153-1159.

192. M. Saifee, N. Inamdar, D.L. Dhamecha and A.A. Rathi, *Int. J. Health Res.*, **2009**, *2*, 291-306.

193. A.J. Aguiar, J. Krc Jr., A.W. Kinkel and J.C. Samyn, *J. Pharm. Sci.*, **1967**, *56*, 847-853.

194. H.G. Brittain, *Spectroscopy*, **2000**, *15*, 34-39.

195. ICH Topic Q6A, Specifications: Test procedures and acceptance criteria for new drug substances and new drug products: chemical substances, European Medicines Agency, **2000**.

196. D.J. Kempf, K.C. Marsh, J.F. Denissen, E. McDonald, S. Vasavanonda, C.A. Flentge, B.E. Green, L. Fino, C.H. Park, X.-P. Kong, N.E. Wideburg, A. Saldivar, L. Ruiz, W.M. Kati, H.L. Sham, T. Robins, K.D. Steward, A. Hsu, J.J. Plattner, J.M. Leonard and D.W. Norbeck, *Proc. Natl. Acad. Sci. USA*, **1995**, *92*, 2484-2488.

197. S.R. Chemburkar, J. Bauer, K. Deming, H. Spiwek, K. Patel, J. Morris, R. Henry, S. Spanton, W. Dziki, W. Porter, J. Quick, P. Bauer, J. Donaubauer, B.A. Narayanan, M. Soldani, D. Riley and K. McFarland, *Org. Proc. Res. Dev.*, **2000**, *4*, 413-417.

198. A. Hill, J. van der Lugt, W. Sawyer and M. Boffito, *AIDS*, **2009**, *23*, 2237-2245.

199. A. Hill, S. Khoo, M. Boffito and D. Back, *J. Acquir. Immune Defic. Syndr.*, **2011**, *58*, 137-138.

200. M.S. Chorghade (ed.), *Drug Discovery and Development, Vol. 2: Drug Development*, John Wiley & Sons, Hoboken, New Jersey, **2007**.

201. J. Bauer, S. Spanton, R. Henry, J. Quick, W. Dziki, W. Porter and J. Morris, *Pharm. Res.*, **2001**, *18*, 859-866.

202. P.T.A. Galek, F.H. Allen, L. Fábián and N. Feeder, *Cryst. Eng. Comm.*, **2009**, *11*, 2634-2639.

203. J.D. Dunitz and J. Bernstein, *Acc. Chem. Res.*, **1995**, *28*, 193-200.

204. http://www.evaluatepharma.com/Universal/View.aspx?type=Story&id=7343 (26.7.2012)

205. S.L. Morissette, S. Soukasene, D. Levinson, M.J. Cima and Ö. Almarsson, *Proc. Natl. Acad. Sci. USA*, **2003**, *100*, 2180-2184.

206. M. Geppi, G. Mollica, S. Borsacchi and C.A. Veracini, *Appl. Spectros. Rev.*, **2008**, *43*, 202-302.

207. R.K. Harris, *J. Pharm. Pharmacol.*, **2007**, *59*, 225-239.

208. R.T. Berendt, D.M. Sperger, P.K. Isbester and E.J. Munson, *Trends Anal. Chem.*, **2006**, *25*, 977-984.

209. R.K. Harris, P.Y. Ghi, H. Puschmann, D.C. Apperley, U.J. Griesser, R.B. Hammond, C. Ma, K.J. Roberts, G.J. Pearce, J.R. Yates and C.J. Pickard, *Org. Proc. Res. Dev.*, **2005**, *9*, 902-910.

210. J.M. Chalmers and P.R. Griffiths (eds.), *Handbook of Vibrational Spectroscopy. Vol. 1.*, John Wiley & Sons Ltd, **2002**.

211. M. Donahue, E. Botonjic-Sehic, D. Wells and C.W. Brown, *Amer. Pharm. Rev.*, **2011**, *14*.

212. S.L. Morissette, Ö. Almarsson, M.L. Peterson, J.F. Remenar, M.J. Read, A.V. Lemmo, S. Ellis, M.J. Cima and C.R. Gardner, *Adv. Drug Del. Rev.*, **2004**, *56*, 275-300.

213. R. Boese, T. Clark and A. Gavezzotti, *Helv. Chim. Acta*, **2003**, *86*, 1085-1100.

214. E. Zolotoyabko, *Basic Concepts of Crystallography*, Wiley-VCH, **2011**.

215. P.W. Atkins, *Physical Chemistry*, Oxford University Press, Oxford, **1998**.

216. R.I. Cooper, A.L. Thompson and D.J. Watkin, *J. Appl. Cryst.*, **2010**, *43*, 1100-1107.

217. M. Lusi and L.J. Barbour, *Cryst. Growth Des.*, **2011**, *11*, 5515-5521.

218. S.C. Gad (ed.), *Pharmaceutical Sciences Encyclopedia: Drug Discovery, Development, and Manufacturing*, John Wiley & Sons Inc., **2010**.

219. P.J. Haines (ed.), *Principles of Thermal Analysis and Calorimetry*, Royal Society of Chemistry, **2002**.

220. D. Giron, *Thermochim. Acta*, **1995**, *248*, 1-59.

221. J.A. McCauley, R.J. Varsolona and D.A. Levorse, *J. Phys. D: Appl. Phys.*, **1993**, *26*, B85-B89.

222. M. Löfman, J. Koivukorpi, V. Noponen, H. Salo and E. Sievänen, *J. Colloid Interface Sci.*, **2011**, *360*, 633-644.

223. S.J. Clark, M.D. Segall, C.J. Pickard, P.J. Hasnip, M.I.J. Probert, K. Refson and M.C. Payne, *Z. Kristallogr.*, **2005**, *220*, 567-570.

224. C.G. Broyden, *J. Inst. Math. Appl.*, **1970**, *6*, 222-231.

225. R. Fletcher, *Comput. J.*, **1970**, *13*, 317-322.

226. D. Goldfarb, *Math. Comp.*, **1970**, *24*, 23-26.

227. D.F. Shanno, *Math. Comp.*, **1970**, *24*, 647-656.

228. J.R. Yates, C.J. Pickard and F. Mauri, *Phys. Rev. B*, **2007**, *76*, 024401-1-024401-11.

229. C.J. Pickard and F. Mauri, *Phys. Rev. B*, **2001**, *63*, 245101-1-245101-13.

230. G. Portalone and M. Colapietro, *Acta Crystallogr. E*, **2007**, *63*, O1869-O1871.

Erratum to I

Table 2 CSA tensor components (ppm) of carbonyl carbon in **2** and **3**

Parameter	2	3
δ_{11}	221.0	219.4
δ_{22}	170.4	175.3
δ_{33}	115.3	119.8
η	0.90	0.85
d	-80.4	-77.5
δ_{iso}	169.0	171.5

Assuming $\delta_{11}>\delta_{22}>\delta_{33}$, $\delta_{iso}=\delta_{11}+\delta_{22}+\delta_{33}$, $\eta=(\delta_{22}-\delta_{11})/\ \delta_{33}-\delta_{iso}$, $d=\delta_{33}-(\delta_{11}+\delta_{22})/2$

Should be:

Table 2 CSA tensor components (ppm) of carbonyl carbon in **2** and **3**

Parameter	2	3
δ_{11}	245.4	243.2
δ_{22}	173.0	177.3
δ_{33}	88.6	94.0
η	0.90	0.85
CSA	-80.4	-77.5
δ_{iso}	169.0	171.5

Assuming $\delta_{11}>\delta_{22}>\delta_{33}$, $\delta_{iso}=(\delta_{11}+\delta_{22}+\delta_{33})/3$, $\eta=(\delta_{22}-\delta_{11})/(\delta_{33}-\delta_{iso})$, $CSA=\delta_{33}-\delta_{iso}$

The term “polymorph” was incorrectly used in this paper, whereas “crystal form” would have been the correct term.

ORIGINAL PAPERS

I

Structural studies on lithocholyl-*N*-(2-aminoethyl)amide in the solid state

by

K. Ahonen, B. Behera, E. Sievänen, A. Valkonen, M. Lahtinen, M. Tolonen, R. Kauppinen and E. Kolehmainen, 2010

Struct. Chem., **2010**, *21*, 185-190. DOI: 10.1007/s11224-009-9560-7

II

Microwave assisted synthesis and solid state characterization of lithocholyl amides of isomeric aminopyridines

by

K. Ahonen, M. Lahtinen, A. Valkonen, M. Dračínský and E. Kolehmainen, 2011

Steroids, **2011**, *76*, 261-268. DOI: 10.1016/j.steroids.2010.11.007

III

Structural studies of five novel bile acid-4-aminopyridine conjugates

by

K. Ahonen, M. Lahtinen, M. Löfman, A. Kiesilä, A. Valkonen, E. Sievänen, Nonappa and E. Kolehmainen, 2012

Steroids, **2012**, *77*, 1141-1151. DOI: 10.1016/j.steroids.2012.06.003

IV

Tautomerism and the protonation/deprotonation of isocytosine in liquid- and solid states studied by NMR spectroscopy and theoretical calculations

by

M. Dračinský, P. Jansa, K. Ahonen and M. Buděšinský, 2011

Eur. J. Org. Chem., **2011**, 1544-1551. DOI: 10.1002/ejoc.201001534

V

NMR crystallography of 2-acylamino-6-[1*H*]-pyridones: solid state NMR, GIPAW computational, and single crystal X-ray diffraction studies

by

B. Ośmiałowski, E. Kolehmainen, S.-M. Ikonen, K. Ahonen and M. Löfman, 2011

J. Mol. Struct., **2011**, *1006*, 678-683. DOI: 10.1016/j.molstruc.2011.10.034